Coherent laser radar performance for general atmospheric refractive turbulence

Rod G. Frehlich and Michael J. Kavaya

The signal-to-noise ratio (SNR) and heterodyne efficiency are investigated for coherent (heterodyne detection) laser radar under the Fresnel approximation and general conditions. This generality includes spatially random fields, refractive turbulence, monostatic and bistatic configurations, detector geometry, and targets. For the first time to our knowledge, the effects of atmospheric refractive turbulence are included by using the path-integral formulation. For general conditions the SNR can be expressed in terms of the direct detection power and a heterodyne efficiency that can be estimated from the laser radar signal. For weak refractive turbulence (small irradiance fluctuations at the target) and under the Markov approximation, it is shown that the assumption of statistically independent paths is valid, even for the monostatic configuration. In the limit of large path-integrated refractive turbulence the SNR can become twice the statistically independent-path result. The effects of the main components of a coherent laser radar are demonstrated by assuming untruncated Gaussians for the transmitter, receiver, and local oscillator. The physical mechanisms that reduce heterodyne efficiency are identified by performing the calculations in the receiver plane. The physical interpretations of these results are compared with those obtained from calculations performed in the target plane.

Key words: Laser radar, lidar, coherent detection, heterodyne detection.

I. Introduction

Remote sensing by using laser radar or light detection and ranging (lidar) systems is flourishing as the optimum and sometimes unique technique for numerous scientific, commercial, and military applications. These applications include the profiling of atmospheric aerosol concentrations; the profiling of atmospheric gases by using multiwavelength differential absorption lidar[1-4] (DIAL); meteorological studies and observations of the atmosphere including humidity, clouds, and aerosols[2]; determination of target range, velocity, and identity; target tracking; detection of dangerous low-altitude wind shear near airports[5]; and the space-based global profiling of tropospheric wind fields.[6,7]

Both incoherent (direct) and coherent (heterodyne) detection laser radar measurements have been demonstrated. However, laser radar systems that operate at wavelengths between 0.4 and 1.4 μm are potentially dangerous to the retina of the human eye. Incoherent laser radar systems, which usually use photomultipliers in the visible wavelength region, become insensitive at wavelengths that are >1 μm, where photocathode materials for photomultipliers cease to be effective. Above 1 μm other detector/preamplifier combinations must be used that are comparatively noisy, thereby reducing the sensitivity of incoherent laser radar measurements. Coherent laser radars have several orders of magnitude more sensitivity in the infrared (IR) wavelength region.[8] In addition to sensitivity, heterodyne detection is required for certain laser radar measurements (e.g., wind and target velocity, velocity width, and velocity spectrum).

Much work has been published on coherent laser radar (CLR) theory.[9-35] During the 1960's and 1970's much of the basic formulation of the CLR signal-to-noise ratio (SNR) was developed by Thomson and co-workers with NASA and NOAA support. Most of this work resides in unpublished contract reports.[36,37] The theory of CLR performance is required if one is to understand the physics of the measurement process, to assess the feasibility of proposed measurements (e.g., through computer simulation), to optimize the design of a system, and to devise new applications.

R. G. Frehlich is with the Cooperative Institute for Research in the Environmental Sciences, University of Colorado, Boulder, Colorado 80309. M. J. Kavaya was with Coherent Technologies, Inc., 3300 Mitchell Lane, Suite 330, Boulder, Colorado 80301 when this work was performed. He is now with the Marshall Space Flight Center, NASA, Mail Code EB23, Huntsville, Alabama 35812-0001.

Recieved 3 August 1990.
0003-6935/91/365325-28$05.00/0.

Ideally the theory uses a minimum of assumptions, clearly states the necessary assumptions and their implications, and provides physical insight. Analytic expressions are particularly desired for obtaining understanding and for ease in performing computer simulations. However, we were unable to find published CLR theory and SNR equations that simultaneously met certain criteria that are necessary to obtain the benefits listed above. Examples of this include papers that (1) presented numerical results instead of analytic solutions[20,27,32–34]; (2) were not applicable to the commonly used monostatic CLR system[15,22,29]; (3) made simplifying assumptions at the start concerning the transmitted field, the receiver optics, the local oscillator (LO) field, or the target, which reduced the generality of the results[15,22,27,29]; (4) assumed far-field or near-field focused conditions[10,15,24,25]; and/or (5) neglected atmospheric refractive turbulence effects.[12,14,16,23,29,33–35] The treatment of near-field, nonfocused conditions and atmospheric refractive turbulence effects is becoming more important as laser radar systems employ shorter wavelengths.[38] Books and review papers in the field[1–4,8,39–48] deal primarily with direct detection, and their discussions of coherent detection do not include our desired theoretical development of an SNR equation. Published comparisons of theoretical and experimental CLR SNR show theoretical exceeding experimental by 5–10 dB.[49–52]

The physics of coherent detection for deterministic fields[53–62] is well understood. The performance of coherent detection for this case has been determined with calculations of SNR and heterodyne efficiency. The theoretical foundations of coherent detection were established by Siegman[10] and his antenna theorem, which was derived under the Fraunhofer approximation (far field). The derivation of CLR performance under the Fresnel approximation (the near and far fields) and the target plane formulation was presented by Rye.[16] The performance of CLR systems in the absence of refractive turbulence has been investigated numerically[23,32–34] to determine optimal parameters. Arbitrary field distributions have been analyzed theoretically with orthogonal Hermite polynomial expansions.[35] The effects of atmospheric refractive turbulence have been investigated by using many approximations, none of which is valid in medium or strong path-integrated refractive-turbulence conditions.

Previous work has considered many CLR geometries and targets. Many parameters have been defined to describe CLR performance in various regimes and under various approximations. Many field normalizations have been proposed to simplify the expressions. The system-dependent contribution of the SNR for uniform diffuse targets has been called optical sensitivity by Zhao *et al.*[33] We use the term coherent responsivity and also add the term direct responsivity for the analogous quantity for direct detection laser radar. These two statistics provide a useful description of CLR performance for random transmitter and LO fields, general detector characteristics, general refractive-turbulence spectra (form and strength), and general targets. The analysis is presented first by using the physical fields and a general formulation that is valid for spatially random fields, refractive turbulence, arbitrary detectors, and general targets. Then the most convenient normalized fields are used to identify the most basic system-dependent contribution (coherent and direct responsivity) for the three classes of detector: the large uniform detector, the finite uniform detector, and the arbitrary detector.

We derive a general theory for the SNR of a coherent detection laser radar based on previous work, using the path-integral formulation (Fresnel approximation), which is valid for any typical path-integrated atmospheric refractive turbulence. The general theory and definitions of useful performance parameters are presented in Section II. This includes a heterodyne efficiency for general conditions and targets that can be estimated from the laser radar signal. The leading order effects of refractive turbulence are discussed in Section III. Analytic expressions are presented in Section IV for the case of untruncated Gaussians for the transmitted field, LO field, and transmitter/receiver optics. The physical interpretations of the receiver plane and target plane calculations are also presented. Comparisons with previous work are contained in Section V, and calculations are presented in Section VI. Conclusions and recommendations follow in Section VII.

Although we present analytical results for only the leading order effects of atmospheric refractive turbulence, we provide the tools to analyze laser radar with general refractive turbulence conditions and a general transmitter, receiver, and detector. All results are presented with units explicitly specified to facilitate calculations for real systems. The many expressions for laser radar performance are essential for understanding CLR systems, especially when atmospheric refractive turbulence is important.

II. Theory

A. Detector Plane

Coherent detection laser radar provides optimal detection sensitivity and Doppler information for wind and other target velocity measurements. The performance of coherent detection has been investigated for ideal conditions, i.e., deterministic beams and shot-noise-limited detectors.[53–62] Two important measures of CLR performance are the SNR and heterodyne efficiency. We derive the CLR SNR and the heterodyne efficiency for a general CLR system and general targets under the Fresnel approximation, using the path-integral formulation.[63–70] This theoretical foundation allows a clear extension to both medium and strong path-integrated atmospheric refractive-turbulence conditions.

The geometry for a CLR system is shown in Fig. 1. The optical scalar field $\psi_T(\mathbf{u}, z, t)[(\mathrm{W\ m^{-2}})^{1/2}]$ of the transmitted laser pulse in a homogeneous medium at

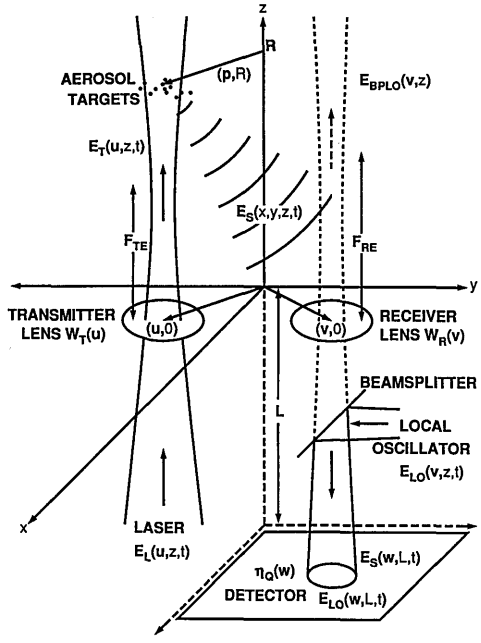

Fig. 1. Geometry for the coherent detection laser radar system. An actual system has an overlap of the transmitted and back propagated local oscillator beams at the target.

transverse coordinate $\mathbf{u}$ (m) and time t (s) is

$$\Psi_T(\mathbf{u}, z, t) = E_T(\mathbf{u}, z, t)\exp(ikz - i\omega t), \quad (1)$$

where $i = \sqrt{-1}$, $k = 2\pi/\lambda$ (rad m^{-1}) is the wave number of the field, λ (m) is the wavelength of the field in a homogeneous medium, $\omega = 2\pi\nu$ (rad s^{-1}) is the angular frequency, ν (Hz) is the optical frequency, and $E_T(\mathbf{u}, z, t)[(W\ m^{-2})^{1/2}]$ is the reduced scalar field. The scalar fields are normalized so that in the absence of extinction

$$\int_{-\infty}^{\infty} \left|\Psi_T(\mathbf{u}, z, t)\right|^2 d\mathbf{u} = \int_{-\infty}^{\infty} \left|E_T(\mathbf{u}, z, t)\right|^2 d\mathbf{u} = P_T(t - z/c), \quad (2)$$

where $|E|$ denotes the absolute value of E, $P_T(t)$ (W) is the transmitted pulse power as a function of time, c (m s^{-1}) is the speed of light in a homogeneous atmosphere, and $d\mathbf{u}$ denotes two-dimensional (2-D) integration over the plane defined by constant z. It is assumed that the pulse profile varies slowly compared with the period of the optical field $1/\nu$. The total backscattered field $\psi_S(\mathbf{v}, z, t)$ is collected by a receiver consisting of an aperture and an effective lens with a dimensionless response function $W_R(\mathbf{v})$, where $\mathbf{v}$ (m) is the transverse coordinate at the receiver plane. The received field is then mixed with a LO field on the surface of a detector at a transverse coordinate $\mathbf{w}$ (m) and distance L (m) from the receiver plane. (A positive L implies a negative z.) The polarization of the LO field is assumed to match that of the backscattered field. (In practice the LO polarization is usually chosen by assuming a nondepolarizing target and a negligible unintentional effect on polarization by the CLR.) The field incident on the detector $\psi_D(\mathbf{w}, L, t)$ is given by

$$\Psi_D(\mathbf{w}, L, t) = E_S(\mathbf{w}, L, t)\exp[i(kL - \omega t + \theta_S)] + E_{LO}(\mathbf{w}, L, t)\exp[i(kL - \omega_{LO}t)], \quad (3)$$

where $E_S(\mathbf{w}, L, t)$ is the reduced backscattered field from the target in the detector plane, $E_{LO}(\mathbf{w}, L, t)$ is the reduced LO field in the detector plane (which may have stationary random fluctuations), ω_{LO} is the angular frequency of the LO, and θ_S (rad) is the random phase of the backscattered field compared with the LO field. The signal current $I(t)$ (A) for an ideal linear detector (e.g., photomultiplier, photodiode) is

$$I(t) = \frac{G_D e}{h\nu} \int_D \eta_Q(\mathbf{w}) |\Psi_D(\mathbf{w}, L, t)|^2 d\mathbf{w}, \quad (4)$$

where $\eta_Q(\mathbf{w})$ (electrons/photon) is the detector quantum efficiency function on the detector surface, G_D is the dimensionless amplifier gain, $e = 1.602 \times 10^{-19}$ (C/electron) is the electronic charge, $h = 6.626 \times 10^{-34}$ (Js) is Planck's constant, and $\int_D$ denotes integration over the detector surface. Substituting Eq. (3) into Eq. (4) produces

$$I(t) = I_{dc}(t) + I_S(t) + i_S(t), \quad (5)$$

where

$$I_{dc}(t) = \frac{G_D e}{h\nu} \int_D \eta_Q(\mathbf{w}) |E_{LO}(\mathbf{w}, L, t)|^2 d\mathbf{w} = \frac{G_D e}{h\nu} P_{LOD} \quad (6)$$

is the direct current (dc) (A) caused by the LO,

$$I_S(t) = \frac{G_D e}{h\nu} \int_D \eta_Q(\mathbf{w}) |E_S(\mathbf{w}, L, t)|^2 d\mathbf{w} = \frac{G_D e}{h\nu} P_D(t) \quad (7)$$

is the direct detection signal current (A) from the backscattered field,

$$i_S(t) = \frac{2G_D e}{h\nu} \mathrm{Re} \int_D \eta_Q(\mathbf{w}) E_S(\mathbf{w}, L, t) E_{LO}^*(\mathbf{w}, L, t)\exp(i\Delta\omega t + i\theta_S) d\mathbf{w} \quad (8)$$

is the intermediate-frequency (i.f.) signal current (A) at frequency $\Delta\omega = \omega_{LO} - \omega \ll \omega$, Re denotes the real part,

$$P_{LOD}(t) = \int_D \eta_Q(\mathbf{w}) |E_{LO}(\mathbf{w}, L, t)|^2 d\mathbf{w} \quad (9)$$

is the effective LO power (W) measured by the detector, and

$$P_D(t) = \int_D \eta_Q(\mathbf{w}) |E_S(\mathbf{w}, L, t)|^2 d\mathbf{w} \quad (10)$$

is the effective direct detection irradiance power (W) measured by the detector. The three components of the signal current are shown in Fig. 2 as a depiction of

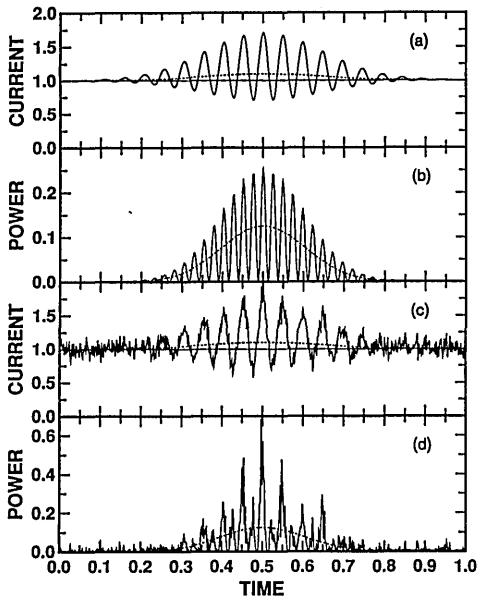

Fig. 2. Depiction of coherent detection signal and power for a Gaussian pulse incident on a rigid hard target: (a) Signal current with no noise and normalized by the average dc $\langle I_{dc}\rangle$. The average backscattered signal current (direct detection current) $\langle I_S(t)\rangle$ is indicated by (----). The i.f. signal is the oscillating component. (b) Intermediate frequency power with no noise (the square of the i.f. signal). The average laser radar power $\langle i_S^2(t)\rangle$ is indicated by (----). (c) Same as (a) but with noise. (d) Same as (b) but with noise. The SNR is 20.0 at time 0.5.

typical data[38,71] from a CLR transmitting a Gaussian pulse and reflected from a rigid target. For typical CLR systems the LO power is much larger than the direct detection power. The i.f. current $i_S(t)$ is obtained by passing the total signal through a bandpass filter to remove the dc and direct detection components and unnecessary noise. The i.f. signal current is converted to power with a squaring circuit (see Fig. 2) and a low-pass filter with bandwidth B (Hz). The average of this CLR power is (see Appendix A)

$$\langle i_S^2(t)\rangle = 2\left(\frac{G_D e}{h\nu}\right)^2 \int_D\int_D \eta_Q(\mathbf{w}_1)\eta_Q(\mathbf{w}_2) M_S(\mathbf{w}_1, \mathbf{w}_2, L, t) \times M_{LO}^*(\mathbf{w}_1, \mathbf{w}_2, L)\,d\mathbf{w}_1 d\mathbf{w}_2, \quad (11)$$

where $\langle\ \rangle$ denotes the ensemble average (or time average for an ergodic process),

$$M_S(\mathbf{w}_1, \mathbf{w}_2, L, t) = \langle E_S(\mathbf{w}_1, L, t) E_S^*(\mathbf{w}_2, L, t)\rangle \quad (12)$$

is the mutual coherence function (W m^{-2}) of the total backscattered field in the detector plane $z = L$, $M_{LO}(\mathbf{w}_1, \mathbf{w}_2, L)$ is the mutual coherence function of the LO field in the detector plane, which is independent of the time t since the LO field is stationary. Here we have assumed that the LO field is statistically independent of the backscattered field. In practice the LO field is usually deterministic, and the random fluctuations of the CLR power are determined from the statistics of the backscattered field.

If the noise is dominated by the LO shot noise[72,73] (an ideal photomultiplier detector or an ideal unbiased photodiode detector), the average noise power (A^2) caused by the Poisson statistics of the detection process is

$$\langle i_N^2\rangle = 2G_D e B\langle I_{dc}\rangle, \quad (13)$$

where $\langle I_{dc}\rangle$ is the average of the dc signal current, Eq. (6), and is also independent of time t since the LO field is stationary. (We assume a photovoltaic detector. Note that a photoconductive detector has a factor of 2 more noise.[8,72]) The dimensionless CLR SNR is defined as (see Fig. 2)

$$\mathrm{SNR}(t) = \frac{\langle i_S^2(t)\rangle}{\langle i_N^2\rangle} = \frac{1}{h\nu B\langle P_{LOD}\rangle}\int_D\int_D \eta_Q(\mathbf{w}_1)\eta_Q(\mathbf{w}_2) M_S(\mathbf{w}_1, \mathbf{w}_2, L, t) \times M_{LO}^*(\mathbf{w}_1, \mathbf{w}_2, L)\,d\mathbf{w}_1 d\mathbf{w}_2, \quad (14)$$

where $\langle P_{LOD}\rangle$ is the average of the effective LO power measured by the detector [see Eq. (9)]. The average i.f. power $\langle i_S^2(t)\rangle$ can be obtained from the following expressions for SNR by multiplying the SNR by the average noise power $\langle i_N^2\rangle$.

Another useful measure of CLR performance is the dimensionless heterodyne efficiency η_H, which measures the loss in coherent power when the received field and the LO field are not perfectly matched. For random fields heterodyne efficiency is defined in an analogous manner to the case of deterministic fields,[24,29,56-62] i.e.,

$$\eta_H(t) = \frac{\langle i_S(t)\rangle}{2\langle I_{dc}\rangle\langle I_S(t)\rangle} = \frac{\int_D\int_D \eta_Q(\mathbf{w}_1)\eta_Q(\mathbf{w}_2) M_S(\mathbf{w}_1, \mathbf{w}_2, L, t) M_{LO}^*(\mathbf{w}_1, \mathbf{w}_2, L)\,d\mathbf{w}_1 d\mathbf{w}_2}{\langle P_D(t)\rangle\langle P_{LOD}\rangle}. \quad (15)$$

The heterodyne efficiency has a maximum value of unity when $E_S(\mathbf{w}, L, t) \propto E_{LO}(\mathbf{w}, L)$. [To see this use the Schwartz inequality, Eq. (9), Eq. (10), and the definition of the mutual coherence function, Eq. (12), in Eq. (15).] The heterodyne efficiency in Eq. (15) can be estimated from the detector signal by using the average CLR power $\langle i_S^2(t)\rangle$ and the ensemble average of the detector current

$$\langle I(t)\rangle = \langle I_{dc}\rangle + \langle I_S(t)\rangle \quad (16)$$

provided the direct detection signal from the backscattered field $I_S(t)$ is large enough to be determined accurately. The average of the direct detection signal $\langle I_S(t)\rangle$ can be obtained by subtracting the average dc $\langle I_{dc}\rangle$ [$\langle I(t)\rangle$ when there is no backscattered signal] from the average signal current $\langle I(t)\rangle$ (see Fig. 2), if the i.f. signal current $i_S(t)$ has a random phase from pulse to pulse or over the observation time. Using a calibration target with high backscatter increases the direct detection signal $I_S(t)$ compared with the dc signal I_{dc} from the LO. The ability to estimate heterodyne efficiency for general conditions provides a useful

measure of the alignment of the backscattered and LO fields on the detector, which is critical to the performance of CLR.

Using Eqs. (14) and (15), we can express the CLR SNR in terms of the heterodyne efficiency as

$$\mathrm{SNR}(t) = \frac{\langle P_D(t)\rangle}{h\nu B}\eta_H(t). \tag{17}$$

The SNR depends on two physical mechanisms: (1) the average direct detection power $\langle P_D(t)\rangle$ and (2) the heterodyne efficiency η_H, in addition to the wavelength λ and detection bandwidth B. Both mechanisms are required to evaluate system performance.

B. Receiver Plane

The propagation of the backscattered field through the receiver complicates CLR calculations. It is more convenient to express the field on the detector in terms of the backscattered field $E_S(\mathbf{v}, 0, t)$ incident on the receiver[16,18,19,54] defined by the plane $z = 0$. The backscattered field after passing through the effective receiver optics (e.g., lens) is expressed in terms of the dimensionless function $W_R(\mathbf{v})$ by

$$E_S(\mathbf{v}, 0-, t) = E_S(\mathbf{v}, 0, t)W_R(\mathbf{v}), \tag{18}$$

where $z = 0-$ defines the plane of an idealized infinitesimally thin receiver aperture. If the Fresnel diffraction approximation is valid, the field on the detector is related to $E_S(\mathbf{v}, 0-, t)$ by

$$E_S(\mathbf{w}, L, t) = \int_{-\infty}^{\infty} E_S(\mathbf{v}, 0-, t)G^f(\mathbf{w}; \mathbf{v}, L)\mathrm{d}\mathbf{v}, \tag{19}$$

where

$$G^f(\mathbf{w}; \mathbf{v}, L) = \frac{k}{2\pi iL}\exp\left[\frac{ik}{2L}(\mathbf{w} - \mathbf{v})^2\right] \tag{20}$$

is the free-space Green's function (m^{-2}). The average of the laser radar power [Eq. (11)] can then be expressed in terms of the fields in the receiver plane, $z = 0$, by substituting Eqs. (12), (18), and (19) into Eq. (11), i.e.,

$$\langle i_S^2(t)\rangle = 2\left[\frac{G_D e}{h\nu}\right]^2 \int_{-\infty}^{\infty}\int_{-\infty}^{\infty} M_S(\mathbf{v}_1, \mathbf{v}_2, 0, t)M_{\mathrm{BPLO}}(\mathbf{v}_1, \mathbf{v}_2, 0)\mathrm{d}\mathbf{v}_1\mathrm{d}\mathbf{v}_2, \tag{21}$$

where

$$E_{\mathrm{BPLO}}(\mathbf{v}, 0) = W_R(\mathbf{v})\frac{k^2}{L^2}\int_{-\infty}^{\infty} E_{\mathrm{LO}}^*(\mathbf{w}, 0)Y[(\mathbf{v} - \mathbf{w})k/L] \times \exp\left[\frac{ik}{2L}(v^2 - w^2)\right]\mathrm{d}\mathbf{w} \tag{22}$$

is the field of the reciprocal receiver[23] or the backpropagated LO (BPLO) field at the target side of the receiver aperture originating from the detector surface, $v^2 = \mathbf{v}\cdot\mathbf{v}$, $w^2 = \mathbf{w}\cdot\mathbf{w}$,

$$Y(\boldsymbol{\kappa}) = \frac{1}{(2\pi)^2}\int_{-\infty}^{\infty}\eta_Q(\mathbf{w})\exp(-i\boldsymbol{\kappa}\cdot\mathbf{w})\mathrm{d}\mathbf{w} \tag{23}$$

is the 2-D Fourier transform (m^2) of the detector quantum efficiency function $\eta_Q(\mathbf{w})$, $\boldsymbol{\kappa}(\mathrm{rad\ m}^{-1})$ is the 2-D wave vector, $E_{\mathrm{LO}}(\mathbf{v}, 0)$ is the LO field at the receiver plane $z = 0$, $M_S(\mathbf{v}_1, \mathbf{v}_2, 0, t)$ ($\mathrm{W\ m}^{-2}$) is the mutual coherence function [see Eq. (12)] of the backscattered field incident on the receiver, and $M_{\mathrm{BPLO}}(\mathbf{v}_1, \mathbf{v}_2, 0)$ is the mutual coherence function of $E_{\mathrm{BPLO}}(\mathbf{v}, 0)$. This representation of the BPLO field defines the receiver of a general CLR including general detector quantum efficiency.

The CLR SNR can be expressed in terms of the backscattered field incident on the receiver and the BPLO field, i.e.,

$$\mathrm{SNR}(t) = \frac{1}{h\nu B\langle P_{\mathrm{LOD}}\rangle}\int_{-\infty}^{\infty}\int_{-\infty}^{\infty} M_S(\mathbf{v}_1, \mathbf{v}_2, 0, t)M_{\mathrm{BPLO}}(\mathbf{v}_1, \mathbf{v}_2, 0)\mathrm{d}\mathbf{v}_1\mathbf{v}_2. \tag{24}$$

This expression is the same as in Eq. (14), except that the calculations are performed in the receiver plane instead of in the detector plane. This eliminates the complexity of propagating the random fields through the receiver. The calculation of the CLR performance in the detector plane provides useful insight.[34] The SNR, the average direct detection power $\langle P_D(t)\rangle$, and the heterodyne efficiency η_H all depend on the CLR components and on the mutual coherence functions of the backscattered and BPLO fields at the plane $z = 0$.

C. Target Plane

The backscattered field at the receiver depends on the transmitted field, the intervening atmosphere, and the nature of the scattering target. The transmitted field incident on a rigid target at transverse coordinate $\mathbf{p}$ (m) and range R (m) in the absence of extinction is

$$E_T(\mathbf{p}, R, t) = \int_{-\infty}^{\infty} E_T(\mathbf{u}, 0, t - R/c)\mathrm{G}(\mathbf{p}; \mathbf{u}, R)\mathrm{d}\mathbf{u}, \tag{25}$$

where $\mathrm{G}(\mathbf{p}; \mathbf{u}, R)$ (m^{-2}) is the Green's function for wave propagation through a turbulent atmosphere with no extinction. We include random fluctuations of the transmitted fields in both space and time over the observation time. This permits analysis of any time-dependent spatial variations of the transmitted field within the pulse. If the transmitted field experiences narrow angular displacement caused by refractive turbulence (the paraxial or Fresnel diffraction approximation), the Green's function is expressed as a Feynman path integral.[63–70] If there is no refractive turbulence, the Green's function is the free-space Green's function, i.e., $\mathrm{G}(\mathbf{p}; \mathbf{u}, R) = G^f(\mathbf{p}; \mathbf{u}, R)$ [see Eq. (20)].

The transmitted field $E_T(\mathbf{u}, 0, t)$ [$(\mathrm{W\ m}^{-2})^{1/2}$] at the

exit of the transmitter aperture is given by

$$E_T(\mathbf{u}, 0, t) = E_L(\mathbf{u}, 0, t)W_T(\mathbf{u}), \tag{26}$$

where $E_L(\mathbf{u}, z, t)$ [(W m^{-2})$^{1/2}$] is the field of the laser, and $W_T(\mathbf{u})$ is the dimensionless response function of the transmitter optics (e.g., lens). All the physics of a laser radar transmitter are described by the effective transmitter field $E_T(\mathbf{u}, 0, t)$. However, the optimal performance of monostatic CLR is referenced to the laser power and requires knowledge of both the laser source field $E_L(\mathbf{u}, z, t)$ and the transmitter response function $W_T(\mathbf{u})$.

The performance of CLR depends on the interaction of the transmitted field with the target. We assume that the backscattered field at the target $E_S(\mathbf{p}, R, t)$ can be expressed as[48]

$$E_S(\mathbf{p}, R, t) = \int_{-\infty}^{\infty} E_T(\mathbf{q}, R, t)V(\mathbf{q}, \mathbf{p})d\mathbf{q}, \tag{27}$$

where $V(\mathbf{q}, \mathbf{p})$ (m^{-2}sr$^{-1/2}$) is the local reflection coefficient of the target. This representation of a hard target allows the special cases of the point scatterer, the dielectric and conductive surface, the diffuse target, and the retroreflector (corner cube). The backscattered field at the receiver in the absence of extinction becomes

$$E_S(\mathbf{v}, 0, t) = \int_{-\infty}^{\infty}\int_{-\infty}^{\infty} E_T(\mathbf{q}, R, t - R/c)V(\mathbf{q}, \mathbf{p})\mathrm{G}(\mathbf{p}; \mathbf{v}, R)d\mathbf{q}d\mathbf{p} \tag{28}$$

on application of the reciprocity theorem for the Green's function,[74] $\mathrm{G}(\mathbf{v}; \mathbf{p}, R) = \mathrm{G}(\mathbf{p}; \mathbf{v}, R)$. If the scattering mechanism of the target is statistically independent of the transmitted field, the mutual coherence function of the total backscattered field in the receiver plane including extinction, and, with the definition of the mutual coherence function, Eqs. (12) and (28), is given by

$$\begin{aligned} M_S(\mathbf{v}_1, \mathbf{v}_2, 0, t) &= [K(R)]^2\langle E_S(\mathbf{v}_1, 0, t)E_S^*(\mathbf{v}_2, 0, t)\rangle \\ &= [K(R)]^2 \int_{-\infty}^{\infty}\int_{-\infty}^{\infty}\int_{-\infty}^{\infty}\int_{-\infty}^{\infty} B(\mathbf{q}_1, \mathbf{q}_2, \mathbf{p}_1, \mathbf{p}_2) \\ &\quad \times \langle E_T(\mathbf{q}_1, R, t - R/c)E_T^*(\mathbf{q}_2, R, t - R/c) \\ &\quad \times \mathrm{G}(\mathbf{p}_1; \mathbf{v}_1, R)\mathrm{G}^*(\mathbf{p}_2; \mathbf{v}_2, R)\rangle d\mathbf{q}_1d\mathbf{q}_2d\mathbf{p}_1d\mathbf{p}_2, \end{aligned} \tag{29}$$

where

$$B(\mathbf{q}_1, \mathbf{q}_2, \mathbf{p}_1, \mathbf{p}_2) = \langle V(\mathbf{q}_1, \mathbf{p}_1)V^*(\mathbf{q}_2, \mathbf{p}_2)\rangle \tag{30}$$

is the target scattering function (m^{-4} sr^{-1}) and

$$K(R) = \exp\left[-\int_0^R \alpha(z)dz\right] \tag{31}$$

is the dimensionless one-way irradiance extinction at wavelength λ, and $\alpha(z)$ (m^{-1}) is the linear extinction coefficient along the propagation path. We neglect any changes in $\alpha(z)$ between transmit and receive paths. When Eq. (25) is substituted into Eq. (28),

$$\begin{aligned} &M_S(\mathbf{v}_1, \mathbf{v}_2, 0, t) \\ &\quad = [K(R)]^2 \int_{-\infty}^{\infty}\int_{-\infty}^{\infty}\int_{-\infty}^{\infty}\int_{-\infty}^{\infty}\int_{-\infty}^{\infty}\int_{-\infty}^{\infty} B(\mathbf{q}_1, \mathbf{q}_2, \mathbf{p}_1, \mathbf{p}_2) \\ &\quad \times M_T(\mathbf{u}_1, \mathbf{u}_2, 0, t - 2R/c)\langle \mathrm{G}(\mathbf{q}_1; \mathbf{u}_1, R)\mathrm{G}^*(\mathbf{q}_2; \mathbf{u}_2, R)\mathrm{G}(\mathbf{p}_1; \mathbf{v}_1, R) \\ &\quad \times \mathrm{G}^*(\mathbf{p}_2; \mathbf{v}_2, R)\rangle d\mathbf{q}_1d\mathbf{q}_2d\mathbf{p}_1d\mathbf{p}_2d\mathbf{u}_1d\mathbf{u}_2, \end{aligned} \tag{32}$$

where $M_T(\mathbf{u}_1, \mathbf{u}_2, z, t)$ is the mutual coherence function of the transmitted field and we have assumed that the transmitted field in the $z = 0$ plane is statistically independent of the random medium. In practice the transmitted field is deterministic at the transmitter lens, and

$$M_T(\mathbf{u}_1, \mathbf{u}_2, 0, t) = E_T(\mathbf{u}_1, 0, t)E_T^*(\mathbf{u}_2, 0, t). \tag{33}$$

However, for partially coherent sources and many unstable-resonator high-powered lasers, the mutual coherence of the transmitter field is required for calculating the SNR and heterodyne efficiency.

The average CLR power $\langle i_S^2(t)\rangle$, SNR, and heterodyne efficiency η_H depend on a special case of the general fourth moment of waves propagating in random media[68] $\langle \mathrm{G}(\mathbf{q}_1; \mathbf{u}_1, R)\mathrm{G}^*(\mathbf{q}_2; \mathbf{u}_2, R)\mathrm{G}(\mathbf{p}_1; \mathbf{v}_1, R)\mathrm{G}^*(\mathbf{p}_2; \mathbf{v}_2, R)\rangle$ [see Eqs. (21) and (32) and on the target-scattering function $B(\mathbf{q}_1, \mathbf{q}_2, \mathbf{p}_1, \mathbf{p}_2)$. Using Eq. (32) for the mutual coherence of the backscattered field in the expression for the SNR [Eq. (24)] results in

$$\begin{aligned} &\mathrm{SNR}(t) \\ &\quad = \frac{[K(R)]^2}{h\nu B\langle P_{\mathrm{LOD}}\rangle} \int_{-\infty}^{\infty}\int_{-\infty}^{\infty}\int_{-\infty}^{\infty}\int_{-\infty}^{\infty}\int_{-\infty}^{\infty}\int_{-\infty}^{\infty}\int_{-\infty}^{\infty}\int_{-\infty}^{\infty} B(\mathbf{q}_1, \mathbf{q}_2, \mathbf{p}_1, \mathbf{p}_2) \\ &\quad \times M_T(\mathbf{u}_1, \mathbf{u}_2, 0, t - 2R/c)M_{\mathrm{BPLO}}(\mathbf{v}_1, \mathbf{v}_2, 0)\langle \mathrm{G}(\mathbf{q}_1; \mathbf{u}_1, R) \\ &\quad \times \mathrm{G}^*(\mathbf{q}_2; \mathbf{u}_2, R)\mathrm{G}(\mathbf{p}_1; \mathbf{v}_1, R)\mathrm{G}^*(\mathbf{p}_2; \mathbf{v}_2, R)\rangle \\ &\quad \times d\mathbf{q}_1d\mathbf{q}_2d\mathbf{p}_1d\mathbf{p}_2d\mathbf{u}_1d\mathbf{u}_2d\mathbf{v}_1d\mathbf{v}_2, \end{aligned} \tag{34}$$

where we have assumed that the transmitted field $E_T(\mathbf{u}, 0, t)$, reciprocal receiver field $E_{\mathrm{BPLO}}(\mathbf{v}, 0)$, and the random medium contribution $\mathrm{G}(\mathbf{p}; \mathbf{u}, R)$ are all statistically independent.

The calculation of SNR or η_H requires an eightfold integration. The order of integration is arbitrary. Performing the $\mathbf{v}$ integrals last results in the receiver plane calculation, Eq. (24). Performing the $\mathbf{q}$ and $\mathbf{p}$ integrals of Eq. (34) last and using Eq. (25) result in the target plane calculation

$$\begin{aligned} \mathrm{SNR}(t) &= \frac{[K(R)]^2}{h\nu B\langle P_{\mathrm{LOD}}\rangle} \int_{-\infty}^{\infty}\int_{-\infty}^{\infty}\int_{-\infty}^{\infty}\int_{-\infty}^{\infty} B(\mathbf{q}_1, \mathbf{q}_2, \mathbf{p}_1, \mathbf{p}_2) \\ &\quad \times \langle E_T(\mathbf{q}_1, R, t - R/c)E_T^*(\mathbf{q}_2, R, t - R/c) \\ &\quad \times E_{\mathrm{BPLO}}(\mathbf{p}_1, R)E_{\mathrm{BPLO}}^*(\mathbf{p}_2, R)\rangle d\mathbf{q}_1d\mathbf{q}_2d\mathbf{p}_1d\mathbf{p}_2 \end{aligned} \tag{35}$$

or, equivalently,

$$\mathrm{SNR}(t) = \frac{[K(R)]^2}{h\nu B\langle P_{\mathrm{LOD}}\rangle} \left\langle \left| \int_{-\infty}^{\infty}\int_{-\infty}^{\infty} V(\mathbf{q}_1, \mathbf{p}_1) \times E_T(\mathbf{q}_1, R, t - R/c)E_{\mathrm{BPLO}}(\mathbf{p}_1, R)d\mathbf{q}_1d\mathbf{p}_1 \right|^2 \right\rangle. \tag{36}$$

(The latter representation is more compact but does not permit ready evaluation since it is not expressed in terms of the basic statistics.) This is the essence of the target plane formulation presented by Rye[18]; the calculations of CLR power can be performed in the target plane by backpropagating the effective LO field to that plane.

D. Targets

1. *Point Scatterer*

For a point scatterer[48] (simple glint)

$$V(\mathbf{q}_1, \mathbf{p}_1) = \lambda \sigma_S^{1/2} \exp(i\theta_S)\delta(\mathbf{q}_1 - \mathbf{p})\delta(\mathbf{p}_1 - \mathbf{p}), \tag{37}$$

$$B(\mathbf{q}_1, \mathbf{q}_2, \mathbf{p}_1, \mathbf{p}_2) = \lambda^2 \sigma_S \delta(\mathbf{p}_1 - \mathbf{p})\delta(\mathbf{p}_2 - \mathbf{p})\delta(\mathbf{q}_1 - \mathbf{p})\delta(\mathbf{q}_2 - \mathbf{p}), \tag{38}$$

where $\mathbf{p}$ (m) is the location of the point scatterer, θ_S (rad) is the phase of the backscattered field, σ_S (m^2 sr^{-1}) is the scattering cross section of the point scatterer, and $\delta(\mathbf{p})$ (m^{-2}) is the 2-D vector δ function. The mutual coherence function of the backscattered field in the receiver plane is

$$M_S(\mathbf{v}_1, \mathbf{v}_2, 0, t) = \lambda^2 \sigma_S [K(R)]^2 \int_{-\infty}^{\infty}\int_{-\infty}^{\infty} M_T(\mathbf{u}_1, \mathbf{u}_2, 0, t - 2R/c) \times \langle G(\mathbf{p}; \mathbf{u}_1, R)G^*(\mathbf{p}; \mathbf{u}_2, R)G(\mathbf{p}; \mathbf{v}_1, R)G^*(\mathbf{p}; \mathbf{v}_2, R)\rangle d\mathbf{u}_1 d\mathbf{u}_2, \tag{39}$$

where we have assumed that the transmitted field and refractive turbulence are statistically independent.

The SNR in the target plane representation is given by

$$\mathrm{SNR}(\mathbf{p}, t) = \frac{\lambda^2 \sigma_S [K(R)]^2}{h\nu B\langle P_{\mathrm{LOD}}\rangle} \langle J_T(\mathbf{p}, R, t - 2R/c) J_{\mathrm{BPLO}}(\mathbf{p}, R)\rangle, \tag{40}$$

where

$$J_T(\mathbf{p}, R, t) = |E_T(\mathbf{p}, R, t)|^2, \qquad J_{\mathrm{BPLO}}(\mathbf{p}, R) = |E_{\mathrm{BPLO}}(\mathbf{p}, R)|^2 \tag{41}$$

are the irradiances (W m^{-2}) of the transmitted field and the BPLO field at range R in the absence of extinction [see Eq. (25)].

2. *Plane Surface*

For a plane deterministic surface (e.g., mirror) whose normal makes an angle θ_P with respect to the transmitter axis,

$$V(\mathbf{q}, \mathbf{p}) = r(\mathbf{p})\delta(\mathbf{q} - \mathbf{p})\exp(2ik\theta_P \cdot \mathbf{p}), \tag{42}$$

$$B(\mathbf{q}_1, \mathbf{q}_2 \mathbf{p}_1, \mathbf{p}_2) = r(\mathbf{p}_1)r^*(\mathbf{p}_2)\exp[2ik\theta_P \cdot (\mathbf{p}_1 - \mathbf{p}_2)]\delta(\mathbf{q}_1 - \mathbf{p}_1)\delta(\mathbf{q}_2 - \mathbf{p}_2), \tag{43}$$

where $r(\mathbf{p})$ ($sr^{-1/2}$) is the complex amplitude reflectivity of the surface. The mutual coherence of the backscattered field at the receiver is then

$$M_S(\mathbf{v}_1, \mathbf{v}_2, 0, t) = [K(R)]^2 \int_{-\infty}^{\infty}\int_{-\infty}^{\infty}\int_{-\infty}^{\infty}\int_{-\infty}^{\infty} r(\mathbf{p}_1)r^*(\mathbf{p}_2) \times \exp[2ik\theta_P \cdot (\mathbf{p}_1 - \mathbf{p}_2)]M_T(\mathbf{u}_1, \mathbf{u}_2, 0, t - 2R/c) \times \langle G(\mathbf{p}_1; \mathbf{u}_1, R)G^*(\mathbf{p}_2; \mathbf{u}_2, R) \times G(\mathbf{p}_1; \mathbf{v}_1, R)G^*(\mathbf{p}_2; \mathbf{v}_2, R)\rangle d\mathbf{p}_1 d\mathbf{p}_2 d\mathbf{u}_1 d\mathbf{u}_2, \tag{44}$$

and the SNR is given by

$$\mathrm{SNR}(t) = \frac{[K(R)]^2}{h\nu B\langle P_{\mathrm{LOD}}\rangle} \int_{-\infty}^{\infty}\int_{-\infty}^{\infty} r(\mathbf{p}_1)r^*(\mathbf{p}_2)\exp[2ik\theta_P(\mathbf{p}_1 - \mathbf{p}_2)] \times \langle E_T(\mathbf{p}_1, R, t - R/c)E_T^*(\mathbf{p}_2, R, t - R/c) \times E_{\mathrm{BPLO}}(\mathbf{p}_1, R)E_{\mathrm{BPLO}}^*(\mathbf{p}_2, R)\rangle d\mathbf{p}_1 d\mathbf{p}_2 \tag{45}$$

in the target plane representation where the fields at the target are calculated in the absence of extinction.

3. *Diffuse-Scattering Target*

For a diffuse-scattering target the reflection coefficient $V(\mathbf{q}, \mathbf{p})$ is random and[48]

$$B(\mathbf{q}_1, \mathbf{q}_2, \mathbf{p}_1, \mathbf{p}_2) = \lambda^2 \rho(\mathbf{p}_1)\delta(\mathbf{p}_1 - \mathbf{p}_2)\delta(\mathbf{q}_1 - \mathbf{p}_1)\delta(\mathbf{q}_2 - \mathbf{p}_2), \tag{46}$$

where $\rho(\mathbf{p})$ (sr^{-1}) is the scattering coefficient at transverse coordinate $\mathbf{p}$. The mutual coherence function of the backscattered field in the receiver plane is

$$M_S(\mathbf{v}_1, \mathbf{v}_2, 0, t) = \lambda^2 [K(R)]^2 \int_{-\infty}^{\infty}\int_{-\infty}^{\infty}\int_{-\infty}^{\infty} \rho(\mathbf{p}) \times M_T(\mathbf{u}_1, \mathbf{u}_2, 0, t - 2R/c) \times \langle G(\mathbf{p}; \mathbf{u}_1, R)G^*(\mathbf{p}; \mathbf{u}_2, R)G(\mathbf{p}; \mathbf{v}_1, R) \times G^*(\mathbf{p}; \mathbf{v}_2, R)\rangle d\mathbf{u}_1 d\mathbf{u}_2 d\mathbf{p}. \tag{47}$$

The SNR in the target plane representation is

$$\mathrm{SNR}(t) = \frac{\lambda^2 [K(R)]^2}{h\nu B\langle P_{\mathrm{LOD}}\rangle} \int_{-\infty}^{\infty} \rho(\mathbf{p})\langle J_T(\mathbf{p}, R, t - 2R/c) J_{\mathrm{BPLO}}(\mathbf{p}, R)\rangle d\mathbf{p} \tag{48}$$

(see Fig. 1 of Ref. 18).

For an infinite uniform diffuse-scattering target $\rho(\mathbf{p}) = \rho$, the average backscattered irradiance in the receiver plane in the absence of turbulence becomes [substitute Eq. (20) into Eq. (47) and integrate]

$$M_S(\mathbf{v}, \mathbf{v}, 0, t) = \frac{\rho}{R^2} [K(R)]^2 \langle P_T(t - 2R/c)\rangle. \tag{49}$$

4. *Retroreflector*

For a retroreflector (corner cube)[48]

$$V(\mathbf{q}, \mathbf{p}) = r(\mathbf{p})\delta(\mathbf{q} + \mathbf{p}), \tag{50}$$

$$B(\mathbf{q}_1, \mathbf{q}_2, \mathbf{p}_1, \mathbf{p}_2) = r(\mathbf{p}_1)r^*(\mathbf{p}_2)\delta(\mathbf{q}_1 + \mathbf{p}_1)\delta(\mathbf{q}_2 + \mathbf{p}_2), \tag{51}$$

where $r(\mathbf{p})$ ($sr^{-1/2}$) is the complex amplitude reflectivity of the surface. The mutual coherence of the

backscattered field at the receiver is then

$$M_S(\mathbf{v}_1, \mathbf{v}_2, 0, t) = [K(R)]^2 \int_{-\infty}^{\infty}\int_{-\infty}^{\infty}\int_{-\infty}^{\infty}\int_{-\infty}^{\infty} r(\mathbf{p}_1) r^*(\mathbf{p}_2) \times M_T(\mathbf{u}_1, \mathbf{u}_2, 0, t - 2R/c) \times \langle G(-\mathbf{p}_1; \mathbf{u}_1, R) G^*(-\mathbf{p}_2; \mathbf{u}_2, R) G(\mathbf{p}_1; \mathbf{v}_1, R) \times G^*(\mathbf{p}_2; \mathbf{v}_2, R)\rangle d\mathbf{p}_1 d\mathbf{p}_2 d\mathbf{u}_1 d\mathbf{u}_2, \quad (52)$$

the SNR is given by

$$\mathrm{SNR}(t) = \frac{[K(R)]^2}{h\nu B\langle P_{LOD}\rangle} \int_{-\infty}^{\infty}\int_{-\infty}^{\infty} r(\mathbf{p}_1) r^*(\mathbf{p}_2) \times \langle E_T(-\mathbf{p}_1, R, t - R/c) E_T^*(-\mathbf{p}_2, R, t - R/c) \times E_{BPLO}(\mathbf{p}_1, R) E_{BPLO}^*(\mathbf{p}_2, R)\rangle d\mathbf{p}_1 d\mathbf{p}_2 \quad (53)$$

in the target plane representation, and the fields at the target are calculated in the absence of extinction.

5. *Distributed Aerosol Target*

The receiver plane calculation of SNR, η_H, and received CLR power $\langle i_S^2(t)\rangle$ requires the mutual coherence function of the backscattered field incident on the receiver. For natural aerosol targets, the phase of the backscattered field at each aerosol particle is random, and the mutual coherence function of the total backscattered field is the addition of the mutual coherence functions from each aerosol particle. The mutual coherence function [see Eq. (12)] of the backscattered field at the receiver because of a single aerosol particle is the same as that for a point scatterer [see Eq. (39)]. The mutual coherence function of the total backscattered field at the receiver is obtained by integrating Eq. (39) over all the scattering aerosols (i.e., over $\mathbf{p}$, R, and σ_S),

$$M_S(\mathbf{v}_1, \mathbf{v}_2, 0, t) = \lambda^2 \int_0^{\infty}\int_{-\infty}^{\infty}\int_{-\infty}^{\infty}\int_{-\infty}^{\infty} \beta(\mathbf{p}, R)[K(R)]^2 \times M_T(\mathbf{u}_1, \mathbf{u}_2, 0, t - 2R/c) \times \langle G(\mathbf{p}; \mathbf{u}_1, R) G^*(\mathbf{p}; \mathbf{u}_2, R) G(\mathbf{p}; \mathbf{v}_1, R) \times G^*(\mathbf{p}; \mathbf{v}_2, R)\rangle d\mathbf{u}_1 d\mathbf{u}_2 d\mathbf{p} dR, \quad (54)$$

where

$$\beta(\mathbf{p}, R) = \int_0^{\infty} \sigma_S N(\sigma_S; \mathbf{p}, R) d\sigma_S \quad (55)$$

is the atmospheric aerosol backscatter coefficient ($\mathrm{m}^{-1}\ \mathrm{sr}^{-1}$) and $N(\sigma_S; \mathbf{p}, R)$ (m^{-5} sr) is the number density of aerosols per unit volume per unit σ_S at location $(\mathbf{p}, R)$. For confined laser beams and typical atmospheric conditions, $\beta(\mathbf{p}, R)$ and $N(\sigma_S; \mathbf{p}, R)$ may be assumed to be functions of range only. Then the average backscattered irradiance in the receiver plane in the absence of refractive turbulence becomes

$$M_S(\mathbf{v}, \mathbf{v}, 0, t) = \int_0^{\infty} \frac{\beta(R)}{R^2} [K(R)]^2 \langle P_T(t - 2R/c)\rangle dR. \quad (56)$$

Note that Eq. (54) has almost the same form as Eq. (47) for a diffuse hard target. All the results for aerosol targets can be converted to diffuse hard target results by replacing $\beta(\mathbf{p}, R)$ with $\rho(\mathbf{p})$ and removing the integration over R. Since the aerosol target results are identical to the diffuse hard target results, a diffuse hard target with a known ρ can be used to calibrate a CLR system for aerosol backscatter measurements.[75-77] In general the calibration measurements must be performed at all ranges of interest. However, if the system geometry is understood, a theoretical calibration curve can be calculated and compared with calibration measurements made at one or more suitable ranges.[76]

The target plane calculation of the SNR is obtained by performing the integration over the target last [substitute Eq. (54) into Eq. 24) and rearrange the integration]. Then

$$\mathrm{SNR}(t) = \frac{\lambda_2}{h\nu B\langle P_{LOD}\rangle} \int_0^{\infty}\int_{-\infty}^{\infty} \beta(\mathbf{p}, R)[K(R)]^2 \times \langle J_T(\mathbf{p}, R, t - R/c) J_{BPLO}(\mathbf{p}, R)\rangle d\mathbf{p} dR, \quad (57)$$

which would be compared with Eq. (48), the diffuse target case.

Note that Eqs. (40), (45), (48), and (57) are symmetric in $E_T(\mathbf{p}, R)$ and $E_{BPLO}(\mathbf{p}, R)$ and are also symmetric in $E_T(\mathbf{u}, 0)$ and $E_{BPLO}(\mathbf{v}, 0)$. Laser radar power, the SNR, and heterodyne efficiency η_H are unchanged with an interchange of $E_T(\mathbf{u}, 0)$ and $E_{BPLO}(\mathbf{v}, 0)$ for a point scatterer, diffuse target, aerosol target, and plane surface. This is not true for the case of a retroreflector target [see Eq. (53)].

E. System Performance: Infinite Uniform Detector

It is convenient to define the system performance by using the most basic system components. This concept was applied to the case of infinite aerosol targets in free space for deterministic fields by Zhao *et al.*[33] We apply this concept for general conditions and general targets. The formulation depends on the three detector geometries: a large uniform detector, a finite uniform detector, and a nonuniform detector. We present explicit results for the first case since this geometry is common and produces familiar expressions. The extension to the last two cases is obtained by appropriate substitutions.

The basic components of system performance are extracted by convenient field normalization. [Some authors normalize the scalar field so that

$$\frac{c\epsilon_0}{2} \int_{-\infty}^{\infty} |E_T(\mathbf{x})|^2 d\mathbf{x} = P_T, \quad (58a)$$

where ϵ_0 (F m^{-1}) is the permittivity of free space and $E_T(\mathbf{x})$ (V m^{-1}) is defined in the mks system of units [compare with Eq. (2)]. Shaprio *et al.*[19] introduced the normalized signal $r(t)$ ($\mathrm{W}^{1/2}$) given by

$$r(t) = \frac{h\nu}{(2P_{LOD})^{1/2} G_D e \eta_Q} i_S(t), \quad (58b)$$

where η_Q is a constant detector quantum efficiency. With this normalization the average shot-noise power for $\langle r^2(t)\rangle$ is $h\nu B/\eta_Q$, which is different from the current noise power [Eq. (13)].] The normalized fields are defined by

$$E_L(\mathbf{u}, z, t) = [\langle P_L(t)\rangle]^{1/2} e_L(\mathbf{u}, z, t), \tag{59}$$

$$E_{\mathrm{LO}}(\mathbf{v}, z) = [\langle P_{\mathrm{LO}}\rangle]^{1/2} e_{\mathrm{LO}}(\mathbf{v}, z), \tag{60}$$

where $e_L(\mathbf{u}, z, t)$ (m^{-1}) and e_{LO} ($\mathbf{v}$, z) (m^{-1}) are the normalized fields for the transmitted laser field and LO field, respectively, and P_{LO} (W) is the total power of the LO beam. This normalization references CLR performance to the average laser power $\langle P_L(t)\rangle$ instead of to the average laser power transmitted $\langle P_T(t)\rangle$.

For a CLR with a detector that has uniform quantum efficiency η_Q and that collects all the energy of both the LO and the backscattered fields incident on the receiver aperture, the Fourier transform of the detector response, Eq. (23), is

$$Y(\boldsymbol{\kappa}) = \eta_Q \delta(\boldsymbol{\kappa}). \tag{61}$$

Then the BPLO field, Eq. (22), becomes

$$E_{\mathrm{BPLO}}(\mathbf{v}, 0) = \eta_Q E_{\mathrm{LO}}^*(\mathbf{v}, 0) W_R(\mathbf{v}), \tag{62}$$

and the average power measured by the detector is

$$\langle P_{\mathrm{LOD}}\rangle = \eta_Q \langle P_{\mathrm{LO}}\rangle. \tag{63}$$

The normalized field at the exit of the transmitter is defined as

$$e_T(\mathbf{u}, 0, t) = e_L(\mathbf{u}, 0, t) W_T(\mathbf{u}), \tag{64}$$

and the normalized field of the BPLO at the exit of the reciprocal receiver is defined as

$$e_{\mathrm{BPLO}}(\mathbf{v}, 0) = e_{\mathrm{LO}}^*(\mathbf{v}, 0) W_R(\mathbf{v}). \tag{65}$$

The performance of CLR can be expressed in terms of these basic normalized fields for general conditions, general atmospheric refractive turbulence, and general targets.

1. *Point Scatterer*

Usings Eqs. (24) and (39) and the normalized fields, we can write the SNR for a point scatterer at $(\mathbf{p}, R)$ as

$$\mathrm{SNR}(t) = \frac{\eta_Q \langle P_L(t - 2R/c)\rangle [K(R)]^2 \sigma_S}{h\nu B} c(\mathbf{p}, R, t), \tag{66}$$

where

$$c(\mathbf{p}, R, t) = \lambda^2 \int_{-\infty}^{\infty}\int_{-\infty}^{\infty}\int_{-\infty}^{\infty}\int_{-\infty}^{\infty} m_T(\mathbf{u}_1, \mathbf{u}_2, 0, t - 2R/c) \times m_{\mathrm{BPLO}}(\mathbf{v}_1, \mathbf{v}_2, 0)\langle \mathrm{G}(\mathbf{p}; \mathbf{u}_1, R)\mathrm{G}^*(\mathbf{p}; \mathbf{u}_2, R) \times \mathrm{G}(\mathbf{p}; \mathbf{v}_1, R)\mathrm{G}^*(\mathbf{p}; \mathbf{v}_2, R)\rangle \mathrm{d}\mathbf{u}_1 \mathrm{d}\mathbf{u}_2 \mathrm{d}\mathbf{v}_1 \mathrm{d}\mathbf{v}_2 \tag{67}$$

is the coherent responsivity density (m^{-2}) of the CLR. Here m_T ($\mathbf{u}_1$, $\mathbf{u}_2$, 0, t) (m^{-2}) and m_{BPLO} ($\mathbf{v}_1$, $\mathbf{v}_2$, 0) (m^{-2}) are the mutual coherence functions [see Eq. (12)] of the normalized transmitted field e_T ($\mathbf{u}$, 0, t) and BPLO field e_{BPLO} ($\mathbf{v}$, 0), respectively. The term density refers to the dependence on the target coordinate $\mathbf{p}$. The target plane representation of the coherent responsivity density is obtained by integrating Eq. (67) over $\mathbf{u}_1$, $\mathbf{u}_2$, $\mathbf{v}_1$, and $\mathbf{v}_2$, i.e.,

$$c(\mathbf{p}, R, t) = \lambda^2 \langle j_T(\mathbf{p}, R, t - R/c) j_{\mathrm{BPLO}}(\mathbf{p}, R)\rangle, \tag{68}$$

where

$$j_T(\mathbf{p}, R, t) = |e_T(\mathbf{p}, R, t)|^2, \qquad j_{\mathrm{BPLO}}(\mathbf{p}, R) = |e_{\mathrm{BPLO}}(\mathbf{p}, R)|^2 \tag{69}$$

are the random irradiances (m^{-2}) of the normalized transmitter and BPLO fields at the target [see Eq. (25)].

The average integrated normalized transmitter irradiance is

$$\int_{-\infty}^{\infty} \langle j_T(\mathbf{u}, 0, t)\rangle \mathrm{d}\mathbf{u} = \langle P_T(t)/P_L(t)\rangle = T_T(t), \tag{70}$$

where $T_T(t)$ is the average fraction of the last power transmitted through the transmitter aperture defined by $W_T(\mathbf{u})$. Similarly, for an infinite, uniform detector, the average integrated normalized BPLO irradiance is

$$\int_{-\infty}^{\infty} \langle j_{\mathrm{BPLO}}(\mathbf{v}, 0)\rangle \mathrm{d}\mathbf{v} = T_R, \tag{71}$$

where T_R is the average fraction of the LO power that would be transmitted through the reciprocal receiver defined by $W_R(\mathbf{v})$.

The SNR can also be expressed [see Eq. (17)] in terms of the average power collected by the detector and the heterodyne efficiency. For a large uniform detector all the power collected by the receiver is measured by the detector. Therefore, the average direct detection power $\langle P_D(t)\rangle$ [see Eq. (10)] can be expressed in terms of the mutual coherence of the backscattered field incident on the receiver, i.e.,

$$\langle P_D(t)\rangle = \eta_Q \int_{-\infty}^{\infty} |W_R(\mathbf{v})|^2 M_S(\mathbf{v}, \mathbf{v}, 0, t) \mathrm{d}\mathbf{v}. \tag{72}$$

For the point scatterer [substitute Eq. (39) into Eq. (72)]

$$\langle P_D(t)\rangle = \eta_Q \langle P_L(t - 2R/c)\rangle [K(R)]^2 \sigma_S d(\mathbf{p}, R, t), \tag{73}$$

where

$$d(\mathbf{p}, R, t) = \lambda^2 \int_{-\infty}^{\infty}\int_{-\infty}^{\infty}\int_{-\infty}^{\infty} m_T(\mathbf{u}_1, \mathbf{u}_2, 0, t - 2R/c) |W_R(\mathbf{v})|^2 \times \langle \mathrm{G}(\mathbf{p}; \mathbf{u}_1, R)\mathrm{G}^*(\mathbf{p}; \mathbf{u}_2, R)\mathrm{G}(\mathbf{p}; \mathbf{v}, R)\mathrm{G}^*(\mathbf{p}; \mathbf{v}, R)\rangle \mathrm{d}\mathbf{u}_1 \mathrm{d}\mathbf{u}_2 \mathrm{d}\mathbf{v} \tag{74}$$

is the direct responsivity density (m^{-2}) of the laser radar. The target plane representation of direct re-

sponsivity density is obtained by integrating Eq. (74) over $\mathbf{u}_1$, $\mathbf{u}_2$, and $\mathbf{v}$, i.e.,

$$d(\mathbf{p}, R, t) = \lambda^2 \langle j_T(\mathbf{p}, R, t - R/c) j_R(\mathbf{p}, R) \rangle, \quad (75)$$

where

$$j_R(\mathbf{p}, R) = \int_{-\infty}^{\infty} |W_R(\mathbf{v})|^2 G(\mathbf{p}; \mathbf{v}, R) G^*(\mathbf{p}; \mathbf{v}, R) d\mathbf{v} \quad (76)$$

is the random irradiance (m^{-2}) of a normalized spatially incoherent source defined by the receiver aperture $|W_R(\mathbf{v})|^2$. The target plane representation of the direct responsivity density is the correlation between the normalized transmitted irradiance and the irradiance from a normalized spatially incoherent source distribution given by the aperture transmittance $|W_R(\mathbf{v})|^2$. By using Eqs. (17), (66), and (73), the heterodyne efficiency for a point scatterer or simple glint target at $(\mathbf{p}, R)$ is

$$\eta_H(\mathbf{p}, R, t) = \frac{c(\mathbf{p}, R, t)}{d(\mathbf{p}, R, t)}. \quad (77)$$

This states that heterodyne efficiency is the fraction of the direct (incoherent) detection power converted to coherent (heterodyne) detection power by the CLR. In the target plane representation the heterodyne efficiency is

$$\eta_H(\mathbf{p}, R, t) = \frac{\langle j_T(\mathbf{p}, R, t - R/c) j_{\mathrm{BPLO}}(\mathbf{p}, R) \rangle}{\langle j_T(\mathbf{p}, R, t - R/c) j_R(\mathbf{p}, R) \rangle}. \quad (78)$$

2. *Infinite Uniform Diffuse Hard Target*

When the backscatter coefficient $\rho(\mathbf{p})$ is uniform over the dimensions of the transmitted beam, the target can be considered an infinite uniform diffuse hard target. Then $\rho(\mathbf{p}) = \rho$ and [use Eq. (47) in Eq. (24)]

$$\mathrm{SNR}(t) = \frac{\eta_Q \langle P_L(t - 2R/c) \rangle [K(R)]^2 \rho}{h\nu B} C(R, t), \quad (79)$$

where

$$C(R, t) = \int_{-\infty}^{\infty} c(\mathbf{p}, R, t) d\mathbf{p} \quad (80)$$

is the dimensionless coherent responsivity of the CLR. The target plane representation of coherent responsivity is obtained by substituting Eq. (68) into Eq. (80), i.e.,

$$C(R, t) = \lambda^2 \int_{-\infty}^{\infty} \langle j_T(\mathbf{p}, R, t - R/c) j_{\mathrm{BPLO}}(\mathbf{p}, R) \rangle d\mathbf{p}. \quad (81)$$

For the diffuse target the average direct detection power $\langle P_D(t) \rangle$ is given by substituting Eq. (47) into Eq. (72) and using the normalized fields

$$\langle P_D(t) \rangle = \eta_Q P_L(t - 2R/c) [K(R)]^2 \rho D(R, t), \quad (82)$$

where

$$D(R, t) = \int_{-\infty}^{\infty} d(\mathbf{p}, R, t) d\mathbf{p} = \lambda^2 \int_{-\infty}^{\infty} \langle j_T(\mathbf{p}, R, t - R/c) j_R(\mathbf{p}, R) \rangle d\mathbf{p} \quad (83)$$

is the dimensionless direct responsivity of the lasar radar. Then

$$\eta_H(R, t) = \frac{C(R, t)}{D(R, t)}. \quad (84)$$

The heterodyne efficiency is again the fraction of direct detection power converted to coherent detection power by the CLR. By using Eqs. (81), (83), and (84), the target plane representation of heterodyne efficiency is

$$\eta_H(R, t) = \frac{\int_{-\infty}^{\infty} \langle j_T(\mathbf{p}, R, t - R/c) j_{\mathrm{BPLO}}(\mathbf{p}, R) \rangle d\mathbf{p}}{\int_{-\infty}^{\infty} \langle j_T(\mathbf{p}, R, t - R/c) j_R(\mathbf{p}, R) \rangle d\mathbf{p}}. \quad (85)$$

For diffuse and aerosol targets in the far-field regime, Rye[23] has described the performance of CLR in terms of an effective coherent receiver area A_{COH} (m^2). For a diffuse target, we define

$$A_{\mathrm{COH}}(R, t) = R^2 C(R, t) = A_{\mathrm{RYE}}(R, t) T_T(t) T_R, \quad (86)$$

where A_{RYE} is the definition used by Rye. The effective coherent receiver area is also given in terms of an antenna gain $G_A(\mathbf{\Phi})$ (m^2 sr^{-1}), i.e.,

$$A_{\mathrm{COH}}(R, t) = \int_{-\infty}^{\infty} G_A(\mathbf{\Phi}, t) d\mathbf{\Phi}, \quad (87)$$

where

$$G_A(\mathbf{\Phi}, t) = R^4 c(\mathbf{\Phi} R, R, t), \quad (88)$$

and $\mathbf{\Phi}$ (rad) is the angle defined by the target coordinate $(\mathbf{p}, R)$ and the transmitter axis under the Fresnel approximation.

3. *Infinite Uniform Aerosol Target*

When the aerosol backscatter coefficient $\beta(\mathbf{p}, R)$ is uniform over the dimensions of the transmitted beam, the target can be considered an infinite uniform aerosol target and $\beta(\mathbf{p}, R) = \beta(R)$. Substituting Eq. (54) into Eq. (24) and using the normalized fields produce

$$\mathrm{SNR}(t) = \frac{\eta_Q}{h\nu B} \int_0^{\infty} \langle P_L(t - 2R/c) \rangle [K(R)]^2 \beta(R) C(R, t) dR. \quad (89)$$

The average direct detection power $\langle P_D(t) \rangle$ is [substitute Eq. (54) into Eq. (72) and use the normalized fields]

$$\langle P_D(t) \rangle = \eta_Q \int_0^{\infty} \langle P_L(t - 2R/c) \rangle [K(R)]^2 \beta(R) D(R, t) dR. \quad (90)$$

The heterodyne efficiency is given by

$$\eta_H(R, t) = \frac{\int_0^\infty \langle P_L(t - 2R/c)\rangle [K(R)]^2 \beta(R) C(R, t) \mathrm{d}R}{\int_0^\infty \langle P_L(t - 2R/c)\rangle [K(R)]^2 \beta(R) D(R, t) \mathrm{d}R}. \quad (91)$$

For sufficiently short laser pulse durations,

$$\mathrm{SNR}(t) = \frac{\eta_Q \beta(R)[K(R)]^2 c \langle U_L\rangle C(R, t)}{2h\nu B}, \quad (92)$$

$$\langle P_D(t)\rangle = \frac{\eta_Q \langle U_L\rangle c}{2} \beta(R)[K(R)]^2 D(R, t), \quad (93)$$

and the heterodyne efficiency η_H is given by Eq. (84) where U_L(J) is the total laser pulse energy, and $R = ct/2$ is the range probed by the leading edge of the pulse at time t.

4. *Infinite Uniform Plane Surface*

When the complex scattering coefficient $r(\mathbf{p})$ of a plane surface is uniform over the dimensions of the transmitted beam, the target can be considered an infinite uniform plane surface. Then $r(\mathbf{p}) = r$ and the SNR is given by [substitute Eq. (44) into Eq. (24) and use the normalized fields]

$$\mathrm{SNR}(t) = \frac{\eta_Q \langle P_L(t - 2R/c)\rangle [K(R)^2 |r|^2}{h\nu B} C(R, t), \quad (94)$$

where the coherent responsivity is given by

$$C(R, t) = \int_{-\infty}^\infty \int_{-\infty}^\infty \exp[2ik\theta_P \cdot (\mathbf{p}_1 - \mathbf{p}_2)] c_J(\mathbf{p}_1, \mathbf{p}_2, R, t) \mathrm{d}\mathbf{p}_1 \mathrm{d}\mathbf{p}_2, \quad (95)$$

$$\begin{aligned} c_J(\mathbf{p}_1, \mathbf{p}_2, R, t) = \lambda^2 \int_{-\infty}^\infty \int_{-\infty}^\infty \int_{-\infty}^\infty \int_{-\infty}^\infty & m_T(\mathbf{u}_1, \mathbf{u}_2, 0, t) \\ & \times m_{\mathrm{BPLO}}(\mathbf{v}_1, \mathbf{v}_2, 0) \\ & \times \langle \mathrm{G}(\mathbf{p}_1; \mathbf{u}_1, R) \mathrm{G}^*(\mathbf{p}_2; \mathbf{u}_2, R) \mathrm{G}(\mathbf{p}_1; \mathbf{v}_1, R) \\ & \times \mathrm{G}^*(\mathbf{p}_2; \mathbf{v}_2, R)\rangle \mathrm{d}\mathbf{u}_1 \mathrm{d}\mathbf{u}_2 \mathrm{d}\mathbf{v}_1 \mathrm{d}\mathbf{v}_2 \end{aligned} \quad (96)$$

is the joint coherent responsivity density (m^{-4}). The target plane representation is [integrate Eq. (96)]

$$\begin{aligned} c_J(\mathbf{p}_1, \mathbf{p}_2, R, t) = \lambda^2 \langle & e_T(\mathbf{p}_1, R, t - R/c) \\ & \times e_T^*(\mathbf{p}_2, R, t - R/c) e_{\mathrm{BPLO}}(\mathbf{p}_1, R) e_{\mathrm{BPLO}}^*(\mathbf{p}_2, R)\rangle. \end{aligned} \quad (97)$$

The average direct detection power $\langle P_D(t)\rangle$ is [substitute Eq. (44) into Eq. (72) and use the normalized fields]

$$\begin{aligned} \langle P_D(t)\rangle = \eta_Q & \langle P_L(t - 2R/c)\rangle [K(R)]^2 |r|^2 \\ & \times \int_{-\infty}^\infty \int_{-\infty}^\infty \exp[2ik\theta_P \cdot (\mathbf{p}_1 - \mathbf{p}_2)] d_J(\mathbf{p}_1, \mathbf{p}_2, R, t) \mathrm{d}\mathbf{p}_1 \mathrm{d}\mathbf{p}_2, \end{aligned} \quad (98)$$

where the direct responsivity is given by

$$D(R, t) = \int_{-\infty}^\infty \int_{-\infty}^\infty d_J(\mathbf{p}_1, \mathbf{p}_2, R, t) \mathrm{d}\mathbf{p}_1 \mathrm{d}\mathbf{p}_2, \quad (99)$$

$$\begin{aligned} d_J(\mathbf{p}_1, \mathbf{p}_2, R, t) = \lambda^2 \int_{-\infty}^\infty \int_{-\infty}^\infty \int_{-\infty}^\infty & m_T(\mathbf{u}_1, \mathbf{u}_2, 0, t) |W_R(\mathbf{v})|^2 \\ & \times \langle \mathrm{G}(\mathbf{p}_1; \mathbf{u}_1, R) \mathrm{G}^*(\mathbf{p}_2; \mathbf{u}_2, R) \mathrm{G}(\mathbf{p}_1; \mathbf{v}, R) G^*(\mathbf{p}_2; \mathbf{v}, R)\rangle \mathrm{d}\mathbf{u}_1 \mathrm{d}\mathbf{u}_2 \mathrm{d}\mathbf{v} \end{aligned} \quad (100)$$

is the joint direct responsivity density (m^{-4}). The heterodyne efficiency for an infinite uniform plane surface is obtained by using Eq. (84).

5. *Infinite Uniform Retroreflector*

When the complex scattering coefficient $r(\mathbf{p})$ of a retroreflector is uniform over the dimensions of the transmitted beam, the target can be considered an infinite uniform retroreflector. Then $r(\mathbf{p}) = r$ and the SNR is given by Eq. (94) [substitute Eq. (52) into Eq. (24) and use the normalized fields] where

$$\begin{aligned} c_J(\mathbf{p}_1, \mathbf{p}_2, R, t) = \lambda^2 \int_{-\infty}^\infty \int_{-\infty}^\infty \int_{-\infty}^\infty \int_{-\infty}^\infty & m_T(\mathbf{u}_1, \mathbf{u}_2, 0, t - 2R/c) \\ & \times m_{\mathrm{BPLO}}(\mathbf{v}_1, \mathbf{v}_2, 0) \\ & \times \langle \mathrm{G}(-\mathbf{p}_1; \mathbf{u}_1, R) \mathrm{G}^*(-\mathbf{p}_2; \mathbf{u}_2, R) \mathrm{G}(\mathbf{p}_1; \mathbf{v}_1, R) \\ & \times \mathrm{G}^*(\mathbf{p}_2; \mathbf{v}_2, R)\rangle \mathrm{d}\mathbf{u}_1 \mathrm{d}\mathbf{u}_2 \mathrm{d}\mathbf{v}_1 \mathrm{d}\mathbf{v}_2 \end{aligned} \quad (101)$$

is the joint coherent responsivity density. The target plane representation is given by [integrate Eq. (101)]

$$\begin{aligned} c_J(\mathbf{p}_1, \mathbf{p}_2, R, t) = \lambda^2 \langle & e_T(-\mathbf{p}_1, R, t - R/c) \\ & \times e_T^*(-\mathbf{p}_2, R, t - R/c) e_{\mathrm{BPLO}}(\mathbf{p}_1, R) e_{\mathrm{BPLO}}^*(\mathbf{p}_2, R)\rangle. \end{aligned} \quad (102)$$

The average direct detection power $\langle P_D(t)\rangle$ is given by Eq. (98) where

$$\begin{aligned} d_J(\mathbf{p}_1, \mathbf{p}_2, R, t) = \lambda^2 \int_{-\infty}^\infty \int_{-\infty}^\infty \int_{-\infty}^\infty & m_T(\mathbf{u}_1, \mathbf{u}_2, 0, t - 2R/c) \\ & \times |W_R(\mathbf{v})|^2 \langle \mathrm{G}(-\mathbf{p}_1; \mathbf{u}_1, R) \mathrm{G}^*(-\mathbf{p}_2; \mathbf{u}_2, R) \\ & \times \mathrm{G}(\mathbf{p}_1; \mathbf{v}, R) \mathrm{G}^*(\mathbf{p}_2; \mathbf{v}, R)\rangle \mathrm{d}\mathbf{u}_1 \mathrm{d}\mathbf{u}_2 \mathrm{d}\mathbf{v} \end{aligned} \quad (103)$$

is the joint direct responsivity density.

6. *Nonuniform Diffuse Hard Target*

A nonuniform diffuse target is described by the scattering coefficient $\rho(\mathbf{p}, R)$. The SNR is [substitute Eq. (47) into Eq. (24) and use the normalized fields]

$$\mathrm{SNR}(t) = \frac{\eta_Q \langle P_L(t - 2R/c)\rangle [K(R)]^2}{h\nu B} \int_{-\infty}^\infty \rho(\mathbf{p}) c(\mathbf{p}, R, t) \mathrm{d}\mathbf{p}. \quad (104)$$

The average direct detection power $\langle P_D(t)\rangle$ is [substitute Eq. (47) into Eq. (72) and use the normalized fields]

$$\langle P_D(t)\rangle = \eta_Q \langle P_L(t - 2R/c)\rangle [K(R)]^2 \int_{-\infty}^\infty \rho(\mathbf{p}) d(\mathbf{p}, R, t) \mathrm{d}\mathbf{p}. \quad (105)$$

The heterodyne efficiency is given by

$$\eta_H(R, t) = \frac{\int_{-\infty}^\infty \rho(\mathbf{p}) c(\mathbf{p}, R, t) \mathrm{d}\mathbf{p}}{\int_{-\infty}^\infty \rho(\mathbf{p}) d(\mathbf{p}, R, t) \mathrm{d}\mathbf{p}}, \quad (106)$$

which is the ratio of the coherent responsivity density weighted by the target-scattering coefficient to the direct responsivity density weighted by the target-scattering coefficient.

7. *Nonuniform Aerosol Target*

A nonuniform aerosol target is described by the backscatter coefficient $\beta(\mathbf{p}, R)$. The SNR is [substitute Eq. (54) into Eq. (24) and use the normalized fields]

$$\mathrm{SNR}(t) = \frac{\eta_Q}{h\nu B}\int_{-\infty}^{\infty}\int_{0}^{\infty}\langle P_L(t - 2R/c)\rangle[K(R)]^2 \times \beta(\mathbf{p}, R)c(\mathbf{p}, R, t)\mathrm{d}R\mathrm{d}\mathbf{p}. \quad (107)$$

The average direct detection power, $\langle P_D(t)\rangle$ is [substitute Eq. (54) into Eq. (72) and use the normalized fields]

$$\langle P_D(t)\rangle = \eta_Q\int_{-\infty}^{\infty}\int_{0}^{\infty}\langle P_L(t - 2R/c)\rangle[K(R)]^2\beta(\mathbf{p}, R)d(\mathbf{p}, R, t)\mathrm{d}R\mathrm{d}\mathbf{p}. \quad (108)$$

The heterodyne efficiency is given by

$$\eta_H(R, t) = \frac{\int_{-\infty}^{\infty}\int_{0}^{\infty}\langle P_L(t - 2R/c)\rangle[K(R)]^2\beta(\mathbf{p}, R)c(\mathbf{p}, R, t)\mathrm{d}R\mathrm{d}\mathbf{p}}{\int_{-\infty}^{\infty}\int_{0}^{\infty}\langle P_L(t - 2R/c)\rangle[K(R)]^2\beta(\mathbf{p}, R)d(\mathbf{p}, R, t)\mathrm{d}R\mathrm{d}\mathbf{p}}, \quad (109)$$

which is the ratio of the coherent responsivity density weighted by the pulse profile, backscatter coefficient, and extinction to the direct responsivity density weighted by the pulse profile, backscatter coefficient, and extinction. For sufficiently short laser pulse durations

$$\mathrm{SNR}(t) = \frac{\eta_Q\langle U_L\rangle c[K(R)]^2}{2h\nu B}\int_{-\infty}^{\infty}\beta(\mathbf{p},R)c(\mathbf{p}, R, t)\mathrm{d}\mathbf{p}, \quad (110)$$

$$\langle P_D(t)\rangle = \frac{\eta_Q\langle U_L\rangle c}{2}[K(R)]^2\int_{-\infty}^{\infty}\beta(\mathbf{p}, R)d(\mathbf{p}, R, t)\mathrm{d}\mathbf{p}. \quad (111)$$

8. *Nonuniform Plane Surface*

A nonuniform plane surface is described by the complex scattering coefficient $r(\mathbf{p})$. The SNR is [substitute Eq. (44) into Eq. (24) and use the normalized fields]

$$\mathrm{SNR}(t) = \frac{\eta_Q\langle P_L(t - 2R/c)\rangle[K(R)]^2}{h\nu B}\int_{-\infty}^{\infty}\int_{-\infty}^{\infty}\cdot r(\mathbf{p}_1)r^*(\mathbf{p}_2) \times \exp[2ik\boldsymbol{\theta}_P\cdot(\mathbf{p}_1 - \mathbf{p}_2)]c_J(\mathbf{p}_1, \mathbf{p}_2, R, t)\mathrm{d}\mathbf{p}_1\mathrm{d}\mathbf{p}_2. \quad (112)$$

The average direct detection power, $\langle P_D(t)\rangle$ is [substitute Eq. (44) into Eq. (72) and use the normalized fields]

$$\langle P_D(t) = \eta_Q\langle P_L(t - 2R/c)\rangle[K(R)]^2 \times \int_{-\infty}^{\infty}\int_{-\infty}^{\infty}r(\mathbf{p}_1)r^*(\mathbf{p}_2) \times \exp[2ik\boldsymbol{\theta}_P^*\cdot(\mathbf{p}_1 - \mathbf{p}_2)]d_J(\mathbf{p}_1, \mathbf{p}_2, R, t)\mathrm{d}\mathbf{p}_1\mathrm{d}\mathbf{p}_2. \quad (113)$$

The heterodyne efficiency is given by

$$\eta_H(R, t) = \frac{\int_{-\infty}^{\infty}\int_{-\infty}^{\infty}r(\mathbf{p}_1)r^*(\mathbf{p}_2)\exp[2ik\boldsymbol{\theta}_P\cdot(\mathbf{p}_1 - \mathbf{p}_2)]c_J(\mathbf{p}_1, \mathbf{p}_2, R, t)\mathrm{d}\mathbf{p}_1\mathrm{d}\mathbf{p}_2}{\int_{-\infty}^{\infty}\int_{-\infty}^{\infty}r(\mathbf{p}_1)r^*(\mathbf{p}_2)\exp[2ik\boldsymbol{\theta}_P\cdot(\mathbf{p}_1 - \mathbf{p}_2)]d_J(\mathbf{p}_1, \mathbf{p}_2, R, t)\mathrm{d}\mathbf{p}_1\mathrm{d}\mathbf{p}_2}, \quad (114)$$

which is the ratio of the joint coherent responsivity density weighted by the target-scattering coefficient and phase gradient to the joint direct responsivity density weighted by the target-scattering coefficient and phase gradient.

9. *Nonuniform Retroreflector*

A nonuniform retroreflector is described by the complex scattering coefficient $r(\mathbf{p})$. The SNR is given by Eqs. (112) and (101). The average direct detection power $\langle P_D(t)\rangle$ is given by Eqs. (113) and (103), and the heterodyne efficiency is given by Eqs. (114), (101), and (103).

F. No Atmospheric Refractive Turbulence and Deterministic Optical Fields

For deterministic optical fields and no refractive turbulence, ensemble averages over the random media and random fields are not required. All the results of the previous section simplify by substituting the free-space Green's function G^f [see Eq. (20)] for the random Green's function G. For example, the coherent responsivity density, Eq. (67), becomes

$$c(\mathbf{p}, R, t) = \lambda^2\int_{-\infty}^{\infty}\int_{-\infty}^{\infty}\int_{-\infty}^{\infty}\int_{-\infty}^{\infty}e_T(\mathbf{u}_1, 0, t - 2R/c) \times e_T^*(\mathbf{u}_2, 0, t - 2R/c)e_{\mathrm{BPLO}}(\mathbf{v}_1, 0)e_{\mathrm{BPLO}}^*(\mathbf{v}_2, 0) \times G^f(\mathbf{p}; \mathbf{u}_1, R)G^{f*}(\mathbf{p}; \mathbf{u}_2, R)G^f(\mathbf{p}; \mathbf{v}_1, R) \times G^{f*}(\mathbf{p}; \mathbf{v}_2, R)\mathrm{d}\mathbf{u}_1\mathrm{d}\mathbf{u}_2\mathrm{d}\mathbf{v}_1\mathrm{d}\mathbf{v}_2. \quad (115)$$

For a uniform diffuse target the direct responsivity [Eq. (83)] becomes

$$D(R, t) = T_T(t)\Omega(R), \quad (116)$$

where

$$\Omega(R) = A_R/R^2 = \lambda^2 j_R(\mathbf{p}, R) \quad (117)$$

is the solid angle (sr) presented by the receiver with an effective area (m^2) of

$$A_R = \int_{-\infty}^{\infty}|W_R(\mathbf{v})|^2\mathrm{d}\mathbf{v}. \quad (118)$$

Then the coherent responsivity becomes [see Eqs. (84), (116), (117)]

$$C(R, t) = \Omega(R)T_T(t)\eta_H(R, t) = \Omega(R)\eta_S(R, t), \quad (119)$$

where [see Eq. (86)]

$$\eta_S(R, t) \equiv T_T(t)\eta_H(R, t) = \frac{A_{COH}(R, t)}{A_R} = \frac{C(R, t)}{\Omega(R)} \quad (120)$$

is the dimensionless system efficiency, which is a measure of the laser radar performance for the fixed transmitter laser power P_L, fixed LO power P_{LO}, fixed transmitter aperture, fixed receiver aperture, and fixed range R. The system efficiency is also valid for atmospheric refractive turbulence and can be estimated from the laser radar signal by estimating the heterodyne efficiency η_H [see Eq. (15)].

For a uniform diffuse target the target plane representation of heterodyne efficiency is [see Eqs. (70), (85), (117)]

$$\eta_H(R,t) = \frac{R^2\lambda^2}{A_R T_T(t)} \int_{-\infty}^{\infty} j_T(\mathbf{p}, R, t - R/c) j_{BPLO}(\mathbf{p}, R)\mathrm{d}\mathbf{p}. \quad (121)$$

The effective coherent receiver area can also be written as an integration over the receiver plane, i.e.,

$$A_{COH}(R,t) = \int_{-\infty}^{\infty} O_T(\mathbf{s}, R, t) O_{BPLO}^*(\mathbf{s}, R)\mathrm{d}\mathbf{s}, \quad (122)$$

where

$$O_T(\mathbf{s}, R, t) = \int_{-\infty}^{\infty} e_T'(\mathbf{u}, R, t) e_T'^*(\mathbf{u} - \mathbf{s}, R, t)\mathrm{d}\mathbf{u} \quad (123)$$

is the dimensionless autocorrelation function of the field

$$e_T'(\mathbf{u}, R, t) = e_T(\mathbf{u}, 0, t)\exp\left(\frac{ik}{2R}u^2\right), \quad (124)$$

and

$$O_{BPLO}(\mathbf{s}, R) = \int_{-\infty}^{\infty} e'_{BPLO}(\mathbf{v}, R) e'^*_{BPLO}(\mathbf{v} - \mathbf{s}, R)\mathrm{d}\mathbf{v} \quad (125)$$

is the dimensionless autocorrelation function of the field

$$e'_{BPLO}(\mathbf{v}, R) = e_{BPLO}(\mathbf{v}, 0)\exp\left(\frac{ik}{2R}v^2\right). \quad (126)$$

This formulation has been used by Rye[16,23] to express CLR performance in terms of effective areas.

G. System Performance: Finite Uniform Detector

A finite detector does not collect all the available LO power or all the backscattered field incident on the receiver. The average LO power measured by the detector [see Eqs. (9) and (23) and propagate the LO field by using Eq. (19)] is then given by

$$\langle P_{LOD}\rangle = \frac{k^2}{L^2}\langle P_{LO}\rangle \int_{-\infty}^{\infty}\int_{-\infty}^{\infty} m_{LO}(\mathbf{v}_1, \mathbf{v}_2, 0) Y[(\mathbf{v}_1 - \mathbf{v}_2)k/L] \times \exp\left[\frac{ik}{2L}(v_1^2 - v_2^2)\right]\mathrm{d}\mathbf{v}_1\mathrm{d}\mathbf{v}_2 \quad (127)$$

in terms of the normalized LO field at the receiver plane. For a finite detector with a uniform quantum efficiency η_Q, the system performance is given by the results of the previous sections with the substitution

$$e_{BPLO}(\mathbf{v}, 0) = \frac{kW_R(\mathbf{v})\int_{-\infty}^{\infty} e_{LO}^*(\mathbf{w}, 0) Y[(\mathbf{v} - \mathbf{w})k/L]\exp\left[\frac{ik}{2L}(v^2 - w^2)\right]\mathrm{d}\mathbf{w}}{L\left[\int_{-\infty}^{\infty}\int_{-\infty}^{\infty} m_{LO}(\mathbf{v}_1, \mathbf{v}_2, 0) Y[(\mathbf{v}_1 - \mathbf{v}_2)k/L]\exp\left[\frac{ik}{2L}(v_1^2 - v_2^2)\right]\mathrm{d}\mathbf{v}_1\mathrm{d}\mathbf{v}_2\right]^{1/2}} \quad (128)$$

for Eq. (65) where

$$\eta_Q(\mathbf{w}) = 1 \text{ on the detector surface,}$$
$$= 0 \text{ off the detector surface} \quad (129)$$

is used in the definition of $Y(\kappa)$ [see Eq. (23)]. The average direct detection power $\langle P_D(t)\rangle$ is given by the results of the previous section with

$$d(\mathbf{p}, R, t) = \frac{\lambda^2 k^2}{L^2}\int_{-\infty}^{\infty}\int_{-\infty}^{\infty}\int_{-\infty}^{\infty}\int_{-\infty}^{\infty} m_T(\mathbf{u}_1, \mathbf{u}_2, 0, t - 2R/c) \times W_R(\mathbf{v}_1)W_R^*(\mathbf{v}_2) Y[(\mathbf{v}_1 - \mathbf{v}_2)k/L] \times \exp\left[\frac{ik}{2L}(v_1^2 - v_2^2)\right]\{G(\mathbf{p}; \mathbf{u}_1, R)G^*(\mathbf{p}; \mathbf{u}_2, R) \times G(\mathbf{p}; \mathbf{v}_1, R)G^*(\mathbf{p}; \mathbf{v}_2, R)\}\mathrm{d}\mathbf{u}_1\mathrm{d}\mathbf{u}_2\mathrm{d}\mathbf{v}_1\mathrm{d}\mathbf{v}_2 \quad (130)$$

for the point scatterer, diffuse target, and aerosol target;

$$d_J(\mathbf{p}_1, \mathbf{p}_2, R, t) = \frac{\lambda^2 k^2}{L^2}\int_{-\infty}^{\infty}\int_{-\infty}^{\infty}\int_{-\infty}^{\infty}\int_{-\infty}^{\infty} m_T(\mathbf{u}_1, \mathbf{u}_2, 0, t - 2R/c) \times W_R(\mathbf{v}_1)W_R^*(\mathbf{v}_2) Y[(\mathbf{v}_1 - \mathbf{v}_2)k/L] \times \exp\left[\frac{ik}{2L}(v_1^2 - v_2^2)\right]\{G(\mathbf{p}_1; \mathbf{u}_1, R) \times G^*(\mathbf{p}_2; \mathbf{u}_2, R)G(\mathbf{p}_1; \mathbf{v}_1, R) \times G^*(\mathbf{p}_2; \mathbf{v}_2, R)\}\mathrm{d}\mathbf{u}_1\mathrm{d}\mathbf{u}_2\mathrm{d}\mathbf{v}_1\mathrm{d}\mathbf{v}_2 \quad (131)$$

for the plane surface; and

$$d_J(\mathbf{p}_1, \mathbf{p}_2, R, t) = \frac{\lambda^2 k^2}{L^2}\int_{-\infty}^{\infty}\int_{-\infty}^{\infty}\int_{-\infty}^{\infty}\int_{-\infty}^{\infty} m_T(\mathbf{u}_1, \mathbf{u}_2, 0, t - 2R/c) \times W_R(\mathbf{v}_1)W_R^*(\mathbf{v}_2) Y[(\mathbf{v}_1 - \mathbf{v}_2)k/L] \times \exp\left[\frac{ik}{2L}(v_1^2 - v_2^2)\right]\{G(-\mathbf{p}_1; \mathbf{u}_1, R) \times G^*(-\mathbf{p}_2; \mathbf{u}_2, R)G(\mathbf{p}_1; \mathbf{v}_1, R) \times G^*(\mathbf{p}_2; \mathbf{v}_2, R)\}\mathrm{d}\mathbf{u}_1\mathrm{d}\mathbf{u}_2\mathrm{d}\mathbf{v}_1\mathrm{d}\mathbf{v}_2 \quad (132)$$

for the retroreflector; and Eq. (129) is used in the definition of $Y(\kappa)$. The ratio of the average detected power with a finite uniform detector to the average detected power with an infinite uniform detector is the fraction of average power collected by the receiver that is measured by a finite uniform detector. This ratio permits CLR performance to be referenced to the average backscattered power collected by the receiver instead of the average power measured by the detector.

H. System Performance: Finite Nonuniform Detector

A finite detector with a nonuniform quantum efficiency $\eta_Q(\mathbf{w})$ combines the optical effects with the detector effects. The system performance is given by the results of the previous section with the uniform quantum efficiency η_Q removed and by using $\eta_Q(\mathbf{w})$ in the definition of $Y(\kappa)$ instead of Eq. (129).

I. Receiver Plane Representation

All the results for coherent responsivity can be represented in terms of the mutual coherence function of the normalized backscattered field at the receiver plane. This permits a clear presentation of the backscatter enhancement effects caused by atmospheric refractive turbulence (see Section III). For the coherent responsivity density [see Eq. (67)]

$$c(\mathbf{p}, R, t) = \int_{-\infty}^{\infty}\int_{-\infty}^{\infty} m_{SD}(\mathbf{p}, \mathbf{v}_1, \mathbf{v}_2, 0, t) m_{\mathrm{BPLO}}(\mathbf{v}_1, \mathbf{v}_2, 0)\mathrm{d}\mathbf{v}_1\mathrm{d}\mathbf{v}_2, \tag{133}$$

where

$$m_{\mathrm{SD}}(\mathbf{p}, \mathbf{v}_1, \mathbf{v}_2, 0, t) = \lambda^2 \int_{-\infty}^{\infty}\int_{-\infty}^{\infty} m_T(\mathbf{u}_1, \mathbf{u}_2, 0, t - 2R/c) \times \langle \mathrm{G}(\mathbf{p}; \mathbf{u}_1, R)\mathrm{G}^*(\mathbf{p}; \mathbf{u}_2, R)\mathrm{G}(\mathbf{p}; \mathbf{v}_1, R)\mathrm{G}^*(\mathbf{p}; \mathbf{v}_2, R)\rangle \mathrm{d}\mathbf{u}_1\mathrm{d}\mathbf{u}_2 \tag{134}$$

is the mutual coherence function density (m^{-4}) of the normalized backscattered field from a point scatterer at location $(\mathbf{p}, R)$. For an infinite uniform diffuse target the coherent responsivity [see Eq. (80)] is given by

$$C(R, t) = \int_{-\infty}^{\infty}\int_{-\infty}^{\infty} m_S(\mathbf{v}_1, \mathbf{v}_2, 0, t) m_{\mathrm{BPLO}}(\mathbf{v}_1, \mathbf{v}_2, 0)\mathrm{d}\mathbf{v}_1\mathrm{d}\mathbf{v}_2, \tag{135}$$

where

$$m_S(\mathbf{v}_1, \mathbf{v}_2, 0, t) = \int_{-\infty}^{\infty} m_{SD}(\mathbf{p}, \mathbf{v}_1, \mathbf{v}_2, 0, t)\mathrm{d}\mathbf{p} \tag{136}$$

is the mutual coherence function (m^{-2}) of the normalized backscattered field.

The joint coherent responsivity density for a plane surface [see Eq. (96)] is given by

$$c_J(\mathbf{p}_1, \mathbf{p}_2, R, t) = \int_{-\infty}^{\infty}\int_{-\infty}^{\infty} m_{SJ}(\mathbf{p}_1, \mathbf{p}_2, \mathbf{v}_1, \mathbf{v}_2, 0, t) \times m_{\mathrm{BPLO}}(\mathbf{v}_1, \mathbf{v}_2, 0)\mathrm{d}\mathbf{v}_1\mathrm{d}\mathbf{v}_2, \tag{137}$$

where

$$m_{SJ}(\mathbf{p}_1, \mathbf{p}_2, \mathbf{v}_1, \mathbf{v}_2, 0, t) = \lambda^2 \int_{-\infty}^{\infty}\int_{-\infty}^{\infty} m_T(\mathbf{u}_1, \mathbf{u}_2, 0, t - 2R/c) \times \langle \mathrm{G}(\mathbf{p}_1; \mathbf{u}_1, R)\mathrm{G}^*(\mathbf{p}_2; \mathbf{u}_2, R) \times \mathrm{G}(\mathbf{p}_1; \mathbf{v}_1, R)\mathrm{G}^*(\mathbf{p}_2; \mathbf{v}_2, R)\rangle \mathrm{d}\mathbf{u}_1\mathrm{d}\mathbf{u}_2 \tag{138}$$

is the joint mutual coherence function density (m^{-4}) of the normalized backscattered field from two-point scatterers at $(\mathbf{p}_1, R)$ and $(\mathbf{p}_2, R)$.

The joint coherent responsivity density for a retroreflector is given by Eq. (137) where

$$m_{SJ}(\mathbf{p}_1, \mathbf{p}_2, \mathbf{v}_1, \mathbf{v}_2, 0, t) = \lambda^2 \int_{-\infty}^{\infty}\int_{-\infty}^{\infty} m_T(\mathbf{u}_1, \mathbf{u}_2, 0, t - 2R/c) \times \langle \mathrm{G}(-\mathbf{p}_1; \mathbf{u}_1, R)\mathrm{G}^*(-\mathbf{p}_2; \mathbf{u}_2; R) \times \mathrm{G}(\mathbf{p}_1; \mathbf{v}_1, R)\mathrm{G}^*(\mathbf{p}_2; \mathbf{v}_2, R)\rangle \mathrm{d}\mathbf{u}_1\mathrm{d}\mathbf{u}_2. \tag{139}$$

The mutual coherence function of the normalized backscattered field contains the physical interpretation of the coherent detection process in the receiver plane.

III. Effects of Atmospheric Refractive Turbulence

Many theoretical techniques of wave propagation in random media have been used to predict the effects of refractive turbulence on CLR performance. Fried[11] used Rytov theory to estimate signal reduction. Yura[15] modified the bistatic results to describe the effects of refractive turbulence. Wang[22] and Murty[27] used the extended Huygens–Fresnel approximation, which is valid only in weak path-integrated refractive-turbulence conditions.[78] Clifford and Wandzura[20] used the phase approximation of the extended Huygens–Fresnel theory, which is an approximate solution.[63,79] Shapiro *et al.*[19] introduced a phase cancellation limit of the extended Huygens–Fresnel approximation, which considers the log-amplitude scintillation as the dominant mechanism. Their theory is also a weak-integrated refractive-turbulence theory. Rye[18] used phenomenological arguments to include the effects of refractive turbulence. None of these theories has been shown to be valid for general path-integrated refractive turbulence.

It has been argued that the correlation of the transmitted and backscattered fields in monostatic systems will produce improved performance because wave-front tilts will be self-correcting.[20,80] Theoretical justification for this hypothesis is based on geometrical optics arguments (e.g., random wedges that produce a square-law structure function description of the random medium) and the extended Huygens–Fresnel approximation. We show that this self-correcting mechanism is negligible for atmospheric refractive turbulence when the irradiance fluctuations on the target are small.

When the angular deviation of propagating waves because of refractive turbulence is small, the propaga-

tion Green's function is given by a Feynman path integral.[61–68] The moments of the random field are then given in terms of the ensemble average of multiple-path integrals. When the fields change slowly with propagation distance, the Markov approximation is valid[81,82] (i.e., the refractive turbulence is uncorrelated in the propagation direction, a good approximation for normal atmospheric conditions[82]), and the fourth-moment Green's function may be expressed as a series.[68] This series has two physical representations: a low-spatial-frequency (lf) behavior and a high-spatial-frequency (hf) behavior.

A. Low-Spatial-Frequency Behavior

The lf behavior is the dominant behavior when intensity fluctuations at the target are small. The first term of this series (indicated by the subscript 0) for the coherent responsivity density is

$$c_0^{\mathrm{lf}}(\mathbf{p}, R, t) = \lambda^2 \int_{-\infty}^{\infty}\int_{-\infty}^{\infty}\int_{-\infty}^{\infty}\int_{-\infty}^{\infty} m_T(\mathbf{u}_1, \mathbf{u}_2, 0, t - 2R/c) \times m_{\mathrm{BPLO}}(\mathbf{v}_1, \mathbf{v}_2, 0)\langle \mathrm{G}(\mathbf{p}; \mathbf{u}_1, R)\mathrm{G}^*(\mathbf{p}; \mathbf{u}_2, R)\rangle \times \langle \mathrm{G}(\mathbf{p}; \mathbf{v}_1, R)\mathrm{G}^*(\mathbf{p}; \mathbf{v}_2, R)\rangle \mathrm{d}\mathbf{u}_1\mathrm{d}\mathbf{u}_2\mathrm{d}\mathbf{v}_1\mathrm{d}\mathbf{v}_2, \tag{140}$$

and the target plane representation is

$$c_0^{\mathrm{lf}}(\mathbf{p}, R, t) = \lambda^2\langle j_T(\mathbf{p}, R, t - R/c)\rangle\langle j_{\mathrm{BPLO}}(\mathbf{p}, R)\rangle. \tag{141}$$

The analogous term for the direct responsivity density is

$$d_0^{\mathrm{lf}}(\mathbf{p}, R, t) = \lambda^2 \int_{-\infty}^{\infty}\int_{-\infty}^{\infty}\int_{-\infty}^{\infty} m_T(\mathbf{u}_1, \mathbf{u}_2, 0, t - 2R/c)|W_R(\mathbf{v})|^2 \times \langle \mathrm{G}(\mathbf{p}; \mathbf{u}_1, R)\mathrm{G}^*(\mathbf{p}; \mathbf{u}_2, R)\rangle \times \langle \mathrm{G}(\mathbf{p}; \mathbf{v}, R)\mathrm{G}^*(\mathbf{p}; \mathbf{v}, R)\rangle \mathrm{d}\mathbf{u}_1\mathrm{d}\mathbf{u}_2\mathrm{d}\mathbf{v}, \tag{142}$$

and the target plane representation is

$$d_0^{\mathrm{lf}}(\mathbf{p}, R, t) = \lambda^2\langle j_T(\mathbf{p}, R, t - R/c)\rangle\langle j_R(\mathbf{p}, R)\rangle. \tag{143}$$

The first term of the lf behavior of the joint coherent responsivity density is given by

$$c_{J0}^{\mathrm{lf}}(\mathbf{p}_1, \mathbf{p}_2, R, t) = \lambda^2 \int_{-\infty}^{\infty}\int_{-\infty}^{\infty}\int_{-\infty}^{\infty}\int_{-\infty}^{\infty} \times m_T(\mathbf{u}_1, \mathbf{u}_2, 0, t - 2R/c)\, m_{\mathrm{BPLO}}(\mathbf{v}_1, \mathbf{v}_2, 0) \times \langle \mathrm{G}(\mathbf{p}_1; \mathbf{u}_1, R)\mathrm{G}^*(\mathbf{p}_2; \mathbf{u}_2, R)\rangle \times \langle \mathrm{G}(\mathbf{p}_1; \mathbf{v}_1, R)\mathrm{G}^*(\mathbf{p}_2; \mathbf{v}_2, R)\rangle \times \mathrm{d}\mathbf{u}_1\mathrm{d}\mathbf{u}_2\mathrm{d}\mathbf{v}_1\mathrm{d}\mathbf{v}_2, \tag{144}$$

and the target plane representation is

$$c_{J0}^{\mathrm{lf}}(\mathbf{p}_1, \mathbf{p}_2, R, t) = \lambda^2\langle e_T(\mathbf{p}_1, R, t - R/c)e_T^*(\mathbf{p}_2, R, t - R/c)\rangle \times \langle e_{\mathrm{BPLO}}(\mathbf{p}_1, R)\, e_{\mathrm{BPLO}}^*(\mathbf{p}_2, R)\rangle. \tag{145}$$

The analogous term for the joint direct responsivity density is

$$d_{J0}^{\mathrm{lf}}(\mathbf{p}_1, \mathbf{p}_2, R, t) = \lambda^2 \int_{-\infty}^{\infty}\int_{-\infty}^{\infty}\int_{-\infty}^{\infty} m_T(\mathbf{u}_1, \mathbf{u}_2, 0, t - 2R/c)|W_R(\mathbf{v})|^2 \times \langle \mathrm{G}(\mathbf{p}_1; \mathbf{u}_1, R)\mathrm{G}^*(\mathbf{p}_2; \mathbf{u}_2, R)\rangle \times \langle \mathrm{G}(\mathbf{p}_1; \mathbf{v}, R)\mathrm{G}^*(\mathbf{p}_2; \mathbf{v}, R)\rangle \mathrm{d}\mathbf{u}_1\mathrm{d}\mathbf{u}_2\mathrm{d}\mathbf{v}. \tag{146}$$

Using the first term of the series is equivalent to assuming that the backscattered field from the target passes through statistically independent refractive turbulence compared with that of the transmitted field. The next (second) term of the path integral expansion contains the Born approximation. (The field experiences single scattering from refractive turbulence eddies, then interferes with the unscattered field.) This implies that the assumption of statistically independent paths is valid for the monostatic configuration if the contribution from the Born approximation is negligible, i.e., if the irradiance fluctuations at the target are small. This can be inferred from the work of Rye[18] for the infinite uniform diffuse target and the special case of the matched transmitter field and reciprocal receiver field (matched monostatic), i.e.,

$$e_T(\mathbf{u}, 0, t) = e_{\mathrm{BPLO}}(\mathbf{u}, 0), \qquad j_T(\mathbf{p}, R, t) = j_{\mathrm{BPLO}}(\mathbf{p}, R), \tag{147}$$

$$c(\mathbf{p}, R) = \lambda^2\langle j_T(\mathbf{p}, R)\rangle^2[1 + \sigma_I^2(\mathbf{p}, R)], \tag{148}$$

where $\sigma_I^2(\mathbf{p}, R)$ is the dimensionless normalized variance of the transmitted irradiance at the target. Since $\sigma_I^2(\mathbf{p}, R)$ is positive, the statistically independent-path result is a lower bound for the SNR, which is proportional to $c(\mathbf{p}, R)$. When the irradiance fluctuations at the target are small, $\sigma_I^2(\mathbf{p}, R)$ can be neglected and the statistically independent-path result is valid. The calculation of the CLR power by using the phase approximation of the extended Huygens–Fresnel theory depends on the ratio of the field coherence length to the dimensions of the transmitter–receiver. This is the same parameter that describes the effects of refractive turbulence for imaging systems. The regime where the effects of refractive turbulence become important for CLR performance cannot be reliably determined by this parameter. In the limit of large path-integrated refractive turbulence, the complex field at the target becomes a joint Gaussian random process.[64,68] Then[68] $\sigma_I^2(\mathbf{p}, R) = 1$, and the SNR is twice the statistically independent-path result for the matched monostatic condition. For moderate path-integrated refractive turbulence, $\sigma_I^2(\mathbf{p}, R)$ can be larger than unity,[83,84] and for typical atmospheric conditions and wavelengths in the visible, $\sigma_I^2(\mathbf{p}, R)$ approaches unity slowly with increased path-integrated refractive turbulence.

The higher terms of the series solution for the fourth-moment Green's function describe the multiple-interference and correlation effects of propagat-

ing back through the same turbulent atmosphere. As the irradiance fluctuations on the target become large, there is an enhancement of the CLR SNR compared with the statistically independent-path calculation if the fluctuations in irradiance at the target from the transmitter and BPLO are correlated. We call this enhancement normal enhancement. If this enhancement causes the SNR to become larger than the SNR with no refractive turbulence (homogeneous atmosphere or vacuum), we call it super enhancement. The fluctuations in irradiance at the target from the transmitter and BPLO have maximum correlation and hence maximum enhancement for the matched condition. Many conditions are created by varying the transmitter and LO parameters. The physical explanation of the enhanced CLR SNR caused by the refractive turbulence is the correlation of irradiance fluctuations at the target plane. The physical explanation of the enhancement in terms of the receiver plane calculation is the enhancement of the backscattered irradiance at the receiver plane centered on the transmitter axis[48] or an increase in the field coherence of the backscattered field. A clear understanding of the effects of atmospheric refractive turbulence on CLR performance requires calculations in both the target plane and receiver plane.

B. High-Spatial-Frequency Behavior

When the propagation of the fields through refractive turbulence results in great intensity fluctuations at the target, a small-scale structure is produced, i.e., high spatial frequencies. The fourth-moment Green's function that describes this structure can be expressed as a series solution. The leading-order term of this series for the coherent responsivity density is [compared with Eq. (140)]

$$c_0^{\mathrm{hf}}(\mathbf{p}, R, t) = \lambda^2 \int_{-\infty}^{\infty}\int_{-\infty}^{\infty}\int_{-\infty}^{\infty} m_T(\mathbf{u}_1, \mathbf{u}_2, 0, t - 2R/c) \times m_{\mathrm{BPLO}}(\mathbf{v}_1, \mathbf{v}_2, 0)\langle \mathrm{G}(\mathbf{p}; \mathbf{u}_1, R)\mathrm{G}^*(\mathbf{p}; \mathbf{v}_2, R)\rangle \times \langle \mathrm{G}(\mathbf{p}; \mathbf{v}_1, R)\mathrm{G}^*(\mathbf{p}; \mathbf{u}_2, R)\rangle \mathrm{d}\mathbf{u}_1\mathrm{d}\mathbf{u}_2\mathrm{d}\mathbf{v}_1\mathrm{d}\mathbf{v}_2, \tag{149}$$

and the target plane representation is

$$c_0^{\mathrm{hf}}(\mathbf{p}, R) = \lambda^2 |\langle e_T(\mathbf{p}, R, t - R/c) e_{\mathrm{BPLO}}(\mathbf{p}, R)\rangle|^2. \tag{150}$$

The analogous term for the direct responsivity density is

$$d_0^{\mathrm{hf}}(\mathbf{p}, R, t) = \lambda^2 \int_{-\infty}^{\infty}\int_{-\infty}^{\infty}\int_{-\infty}^{\infty} m_T(\mathbf{u}_1, \mathbf{u}_2, 0, t - R/c)|W_R(\mathbf{v})|^2 \times \langle \mathrm{G}(\mathbf{p}; \mathbf{u}_1, R)\mathrm{G}^*(\mathbf{p}; \mathbf{v}, R)\rangle \times \langle \mathrm{G}(\mathbf{p}; \mathbf{v}, R)\mathrm{G}^*(\mathbf{p}; \mathbf{u}_2, R)\rangle \mathrm{d}\mathbf{u}_1\mathrm{d}\mathbf{u}_2\mathrm{d}\mathbf{v}. \tag{151}$$

The first term of the hf behavior of the joint coherent responsivity density is given by

$$c_{J0}^{\mathrm{hf}}(\mathbf{p}_1, \mathbf{p}_2, R, t) = \lambda^2 \int_{-\infty}^{\infty}\int_{-\infty}^{\infty}\int_{-\infty}^{\infty}\int_{-\infty}^{\infty} \times m_T(\mathbf{u}_1, \mathbf{u}_2, 0, t - 2R/c)m_{\mathrm{BPLO}}(\mathbf{v}_1, \mathbf{v}_2, 0) \times \langle \mathrm{G}(\mathbf{p}_1; \mathbf{u}_1, R)\mathrm{G}^*(\mathbf{p}_2; \mathbf{v}_2, R)\rangle \times \langle \mathrm{G}(\mathbf{p}_1; \mathbf{v}_1, R)\mathrm{G}^*(\mathbf{p}_2; \mathbf{u}_2, R)\rangle \mathrm{d}\mathbf{u}_1\mathrm{d}\mathbf{u}_2\mathrm{d}\mathbf{v}_1\mathrm{d}\mathbf{v}_2, \tag{152}$$

and the target plane representation is

$$c_{J0}^{\mathrm{hf}}(\mathbf{p}_1, \mathbf{p}_2, R, t) = \lambda^2 |\langle e_T(\mathbf{p}_1, R, t - R/c) e_{\mathrm{BPLO}}(\mathbf{p}_2, R)\rangle|^2. \tag{153}$$

The analogous term for the joint direct responsivity density is

$$d_{J0}^{\mathrm{hf}}(\mathbf{p}_1, \mathbf{p}_2, R, t) = \lambda^2 \int_{-\infty}^{\infty}\int_{-\infty}^{\infty}\int_{-\infty}^{\infty} m_T(\mathbf{u}_1, \mathbf{u}_2, 0, t - 2R/c) \times |W_R(\mathbf{v})|^2\langle \mathrm{G}(\mathbf{p}_1; \mathbf{u}_1, R)\mathrm{G}^*(\mathbf{p}_2; \mathbf{v}, R)\rangle \times \langle \mathrm{G}(\mathbf{p}_1; \mathbf{v}, R)\mathrm{G}^*(\mathbf{p}_2; \mathbf{u}_2, R)\rangle \mathrm{d}\mathbf{u}_1\mathrm{d}\mathbf{u}_2\mathrm{d}\mathbf{v}. \tag{154}$$

These leading-order effects of refractive turbulence can also be obtained by assuming that the complex fields at the target are a joint Gaussian random process (full saturation of intensity fluctuations). Then the fourth-moment Green's function can be expressed as the sum of the product of the second-moment Green's functions, i.e.,

$$\begin{aligned}\langle \mathrm{G}(\mathbf{p}_1; \mathbf{u}_1, R)\mathrm{G}^*(\mathbf{p}_2; \mathbf{u}_2, R)\mathrm{G}(\mathbf{p}_1; \mathbf{v}_1, R)\langle \mathrm{G}^*(\mathbf{p}_2; \mathbf{v}_2, R)\rangle \\ = \langle \mathrm{G}(\mathbf{p}_1; \mathbf{u}_1, R)\mathrm{G}^*(\mathbf{p}_2; \mathbf{u}_2, R)\rangle\langle \mathrm{G}(\mathbf{p}_1; \mathbf{v}_1, R)\mathrm{G}^*(\mathbf{p}_2; \mathbf{v}_2, R)\rangle \\ + \langle \mathrm{G}(\mathbf{p}_1; \mathbf{u}_1, R)\mathrm{G}^*(\mathbf{p}_2; \mathbf{v}_2, R)\rangle\langle \mathrm{G}(\mathbf{p}_1; \mathbf{v}_1, R)\mathrm{G}^*(\mathbf{p}_2; \mathbf{u}_2, R)\rangle.\end{aligned} \tag{155}$$

The first term in Eq. (155) describes the zero-order term of the lf behavior, and the second term describes the zero-order term of the hf behavior. Then

$$c(\mathbf{p}, R, t) = c_0^{\mathrm{lf}}(\mathbf{p}, R, t) + c_0^{\mathrm{hf}}(\mathbf{p}, R, t), \tag{156}$$

$$d(\mathbf{p}, R, t) = d_0^{\mathrm{lf}}(\mathbf{p}, R, t) + d_0^{\mathrm{hf}}(\mathbf{p}, R, t), \tag{157}$$

$$c_J(\mathbf{p}_1, \mathbf{p}_2, R, t) = c_{J0}^{\mathrm{lf}}(\mathbf{p}_1, \mathbf{p}_2, R, t) + c_{J0}^{\mathrm{hf}}(\mathbf{p}_1, \mathbf{p}_2, R, t), \tag{158}$$

$$d_J(\mathbf{p}_1, \mathbf{p}_2, R, t) = d_{J0}^{\mathrm{lf}}(\mathbf{p}_1, \mathbf{p}_2, R, t) + d_{J0}^{\mathrm{hf}}(\mathbf{p}_1, \mathbf{p}_2, R, t). \tag{159}$$

This approximation was verified previously with path-integral methods.[64–66,68] The limit of full saturation depends on the statistics of the refractive turbulence and the parameters of the transmitter and LO fields. The two terms of the Gaussian field approximations for the fourth-moment Green's function are the basis of the lf series and the hf series.

C. Zero-Order Fourth-Moment Solution

The lf series is required for any strength of path-integrated refractive turbulence. The hf series is important when the intensity fluctuations at the target become large, and small-scale scintillation

structures are formed. The zero-order fourth-moment expressions for the effects of refractive turbulence are given in terms of the second-moment Green's functions ($\langle GG^* \rangle$) for wave propagation in random media.[68] For narrow angular deviations caused by refractive turbulence and the Markov approximation,[81,82]

$$\langle G(\mathbf{p}_1; \mathbf{u}_1, R) G^*(\mathbf{p}_2; \mathbf{u}_2, R) \rangle = \frac{k^2}{(2\pi R)^2} \exp\left\{\frac{ik}{2R}[(\mathbf{p}_1 - \mathbf{u}_1)^2 - (\mathbf{p}_2 - \mathbf{u}_2)^2]\right\} \times \exp\left\{-\frac{1}{2}\int_0^R D'[(\mathbf{u}_1 - \mathbf{u}_2)(1 - z/R) + (\mathbf{p}_1 - \mathbf{p}_2)z/R, z]\mathrm{d}z\right\}, \quad (160)$$

where

$$D'[\mathbf{x}, z] = 4\pi k^2 \int_{-\infty}^{\infty} [1 - \cos(\boldsymbol{\kappa} \cdot \mathbf{x})]\Phi_n(\boldsymbol{\kappa}, \kappa_z = 0, z)\mathrm{d}\boldsymbol{\kappa} \quad (161)$$

is the structure function density (m^{-1}), $\Phi_n(\boldsymbol{\kappa}, \kappa_z, z)$ (m^3) is the local 3-D spectrum of refractive-index fluctuations at range z, and $\boldsymbol{\kappa}$ (rad m^{-1}) is the spectral wave vector. The spectrum is defined by

$$\Phi_n(\boldsymbol{\kappa}, \kappa_z, z) = \frac{1}{(2\pi)^3}\int_{-\infty}^{\infty} B_n(\mathbf{r}, s, z)\exp(-i\boldsymbol{\kappa} \cdot \mathbf{r} - i\kappa_z s)\mathrm{d}\mathbf{r}\mathrm{d}s, \quad (162)$$

where

$$B_n(\mathbf{r}, s, z) = \langle n(\mathbf{p}, z)n(\mathbf{p} + \mathbf{r}, z + s)\rangle \quad (163)$$

is the dimensionless correlation of refractive-index fluctuations $n(\mathbf{p}, z)$ at range z. For Kolmogorov turbulence[85]

$$\int_0^R D'[(\mathbf{u}_1 - \mathbf{u}_2)(1 - z/R), z]\mathrm{d}z = \left[\frac{|\mathbf{u}_1 - \mathbf{u}_2|}{\rho_0(R)}\right]^{5/3}, \quad (164)$$

where

$$\rho_0(R) = [Hk^2 \int_0^R C_n^2(z)(1 - z/R)^{5/3}\mathrm{d}z]^{-3/5} \quad (165)$$

is the transverse-field coherence length (m) of a point source located at $(0, R)$, $C_n^2(z)$ ($\mathrm{m}^{-2/3}$) is the refractive-index structure constant at range z, $H = 2.914383$, and the range integrations in Eqs. (164) and (165) proceed from the laser radar to the scattering volume. Replacing the 5/3 index with 2 in Eq. (165) is a useful approximation that produces little error.[15] This approximation becomes exact[85,86] when the transverse-field coherence length is smaller than the inner scale of the refractive turbulence. Then the average beam profile caused by refractive turbulence is a Gaussian. Note that our theory was *not* developed under a square-law structure function approximation. That pathological case corresponds to an atmosphere composed of random wedges,[80] which implies that there is only beam wander and no scintillation, and wavefront tilts are self-correcting for monostatic lidar.

Using Eqs. (76), (143), and (160),

$$d_0^{\mathrm{lf}}(\mathbf{p}, R, t) = \Omega(R)\langle j_T(\mathbf{p}, R, t - R/c)\rangle. \quad (166)$$

Using Eqs. (70), (83), and (166),

$$D_0^{\mathrm{lf}}(R, t) = T_T(t)\Omega(R), \quad (167)$$

which is the result for no refractive turbulence. The SNR reduction based on the leading term of the lf series is due to a loss in heterodyne efficiency only and not to changes in direct detection power [see Eq. (84)].

For collimated and diverged laser beams the magnitude of the irradiance fluctuations is described by the dimensionless parameter

$$U(R) = \frac{R_F^2}{\rho_0^2(R)} = \frac{R_S(R)}{\rho_0(R)}, \quad (168)$$

where $R_F = (R/k)^{1/2}$ (m) is the Fresnel distance and $R_S(R) = R/[k\rho_0(R)]$ (m) is the radius of the effective scattering region. When U is small the irradiance fluctuations are small[83,85] [$\sigma_I(\mathbf{p}, R) \ll 1$]. When U is extremely large, the irradiance fluctuations are saturated[83,85] [$\sigma_I(\mathbf{p}, R) = 1$], and the CLR performance is given by Eqs. (156–159). These limits provide the following convenient heuristic algorithm for merging the lf behavior with the hf behavior:

$$C_0(R, t) = C_0^{\mathrm{lf}}(R, t) + \frac{U(R)^2}{1 + U(R)^2} C_0^{\mathrm{hf}}(R, t), \quad (169)$$

$$D_0(R, t) = D_0^{\mathrm{lf}}(R, t) + \frac{U(R)^2}{1 + U(R)^2} D_0^{\mathrm{hf}}(R, t), \quad (170)$$

which also provides a connection formula for the heterodyne efficiency η_H. For focused beams in the near-field region the level of scintillation is governed by a different parameter, and the full saturation regime [$\sigma_I(\mathbf{p}, R) = 1$] is approached much sooner.

IV. Gaussian Lidar System

The results presented up to this point are valid for general CLR parameters and conditions (e.g., monostatic and bistatic). The behavior of the laser radar performance in the different physical regimes is more easily described with analytic expressions for SNR and heterodyne efficiency. This section employs complex Gaussian functions for all the main components of a CLR, since this is the simplest representation that still contains all the physics of the system and permits analytic solutions. The physics of the SNR and heterodyne efficiency are described completely by the transmitter field at the exit of the transmitter aperture, the receiver lens, and the LO field.

The remainder of this paper assumes the simplifying assumptions that the transmitter and LO fields are deterministic, that the detector response function is uniform [$\eta_Q(\mathbf{w}) = \eta_Q$], and that the detector col-

lects all the LO power and backscattered power incident on the receiver aperture.

To describe the interaction of the transmitter optics with the laser field (truncation and focusing), we assume an untruncated Gaussian for the transmitter laser, i.e.,

$$e_L(\mathbf{u}, 0, t) = (\pi\sigma_L^2)^{-1/2} \exp\left(-\frac{u^2}{2\sigma_L^2} - \frac{iku^2}{2F_L}\right), \tag{171}$$

where u^2 is $\mathbf{u} \cdot \mathbf{u}$, σ_L (m) is the $1/e$ intensity radius of the laser beam, and F_L (m) is the phase curvature of the laser beam. (F_L is positive if focused at a positive distance z.) [The e^{-2} (14%) intensity diameter is given by $2\sqrt{2}\,\sigma_L$. Truncation effects by a circular aperture, e.g., a mirror, may be safely neglected if the physical aperture diameter is $> 4\sqrt{2}\,\sigma_L$.[87] A circular aperture of radius σ_L passes 63% of the beam power, and a circular aperture of radius $1.5\sqrt{2}\,\sigma_L$ passes 99% of the beam power.] We also assume a monostatic CLR with a transmitter lens described by an untruncated Gaussian response function for the scalar field

$$W_T(\mathbf{u}) = \exp\left(-\frac{u^2}{2\sigma_T^2} - \frac{iku^2}{2F_T}\right), \tag{172}$$

where σ_T (m) is the $1/e$ intensity radius of the transmitter lens and F_T (m) is the phase curvature of the transmitter lens (F_T is positive for a focusing or positive lens.) The untruncated Gaussian assumption, while not as realistic as a circular aperture, allows analytic solutions while preserving a size parameter for the transmitter and receiver components. The normalized field at the exit of the transmitter lens is given by

$$e_T(\mathbf{u}, 0) = (\pi\sigma_L^2)^{-1/2} \exp\left(-\frac{u^2}{2\sigma_{TE}^2} - \frac{iku^2}{2F_{TE}}\right), \tag{173}$$

with

$$\frac{1}{\sigma_{TE}^2} = \frac{1}{\sigma_L^2} + \frac{1}{\sigma_T^2}, \tag{174}$$

where σ_{TE} (m) is the $1/e$ intensity radius of the transmitted field and with

$$\frac{1}{F_{TE}} = \frac{1}{F_L} + \frac{1}{F_T}, \tag{175}$$

where F_{TE} (m) is the phase curvature of the transmitted beam (F_{TE} is positive if focused at a positive distance z.) For the Gaussian transmitter the average irradiance of the normalized transmitted field at the target plane, Eq. (69), becomes

$$\langle j_T(\mathbf{p}, R)\rangle = \frac{\sigma_{TE}^2}{\pi\sigma_L^2\sigma_{BT}^2(R)} \exp\left(-\frac{p^2}{\sigma_{BT}^2(R)}\right), \tag{176}$$

where

$$\sigma_{BT}^2(R) = \sigma_{TE}^2(1 - R/F_{TE})^2 + \frac{R^2}{k^2\sigma_{TE}^2} + \frac{2R^2}{k^2\rho_0^2(R)}. \tag{177}$$

The ensemble average of the normalized irradiance in the target plane has a Gaussian profile with a $1/e$ irradiance radius of σ_{BT} (m).

A. Low-Spatial-Frequency Calculation

The calculation of the CLR performance in the receiver plane requires the mutual coherence function of the normalized backscattered field at the receiver. The first term of the lf behavior is [using Eqs. (133), (134), (136), (140), and (160) and the square-law approximation for the structure function]

$$m_{S_0}^{lf}(\mathbf{v}_1, \mathbf{v}_2, 0) = \frac{\sigma_{TE}^2}{\sigma_L^2 R^2} \exp\left[\frac{ik}{R}\mathbf{r} \cdot \mathbf{s} - \frac{s^2}{2\rho_0^2(R)} - \frac{s^2\sigma_{BT}^2(R)k^2}{4R^2}\right], \tag{178}$$

where

$$2\mathbf{r} = \mathbf{v}_1 + \mathbf{v}_2, \qquad \mathbf{s} = \mathbf{v}_1 - \mathbf{v}_2 \tag{179}$$

are the centroid and difference coordinates (m), respectively. The term $(ik/R)\mathbf{r} \cdot \mathbf{s}$ represents the phase-front curvature of the backscattered fields. The term $s^2/[2\rho_0^2(R)]$ is the one-way loss of the field coherence of the backscattered fields because of refractive turbulence, and the last term in the exponent is the loss of field coherence because of the propagation of the fields from the illuminated target (defined by the average irradiance of the transmitted beam) back to the receiver in the absence of refractive turbulence.

For spatially varying irradiance the field coherence length is defined by the complex degree of coherence[88]

$$\hat{m}(\mathbf{v}_1, \mathbf{v}_2, 0) = \frac{m(\mathbf{v}_1, \mathbf{v}_2, 0)}{[m(\mathbf{v}_1, \mathbf{v}_1, 0)m(\mathbf{v}_2, \mathbf{v}_2, 0)]^{1/2}}. \tag{180}$$

For the leading-order term

$$\hat{m}_{S_0}^{lf}(\mathbf{v}_1, \mathbf{v}_2, 0) = \exp\left[\frac{ik}{R}\mathbf{r} \cdot \mathbf{s} - \frac{s^2}{2\hat{\rho}_0^2(R)}\right], \tag{181}$$

where

$$\frac{1}{\hat{\rho}_0^2(R)} = \frac{1}{\rho_0^2(R)} + \frac{\sigma_{BT}^2(R)k^2}{2R^2} \tag{182}$$

is the effective field coherence length at the receiver axis and describes the leading-order behavior of the small-scale coherence at the receiver caused by the large-scale structure of the target. The first term in Eq. (182) is the field coherence of a point source at the target propagating through the refractive turbulence. The second term is the field coherence caused by the free-space propagation of a spatially incoherent source defined by the average transmitted irradiance $j_T(\mathbf{p}, R)$. This is the Van Cittert–Zernike theorem.[88]

The average irradiance of the normalized backscattered field is given by

$$m_{S_0}^{\text{lf}}(\mathbf{v}, \mathbf{v}, 0) = \frac{\sigma_{\text{TE}}^2}{\sigma_L^2 R^2}, \tag{183}$$

which is independent of the level of the refractive turbulence. This is not true for the other terms of the path-integral expansions, which describe the backscatter enhancement mechanism.

We assume a monostatic CLR with a receiver lens described by an untruncated Gaussian receiver response function [see Eq. (172)] for the scalar field:

$$W_R(\mathbf{v}) = \exp\left(-\frac{v^2}{2\sigma_R^2} - \frac{ikv^2}{2F_R}\right), \tag{184}$$

where σ_R (m) is the $1/e$ intensity radius of the receiver, and F_R (m) is the phase curvature (the focal length of the lens or telescope) of the receiver (F_R is positive for a focusing or positive lens.) [Although actual lidar systems usually employ a rectangular top hat receiver function (e.g., a circular telescope primary mirror), the Gaussian assumption allows analytic solutions while preserving a size parameter for the receiver. Gaussian profile truncation by the receiver is therefore included unless we set $\sigma_R \to \infty$, in which case there is no receiver truncation. The same comments apply to the transmitter function and σ_T.] The effective receiver area $A_R = \pi\sigma_R^2$ [see Eq. (118)].

The LO at the receiver plane ($z = 0$) is assumed to be an untruncated Gaussian beam, i.e.,

$$e_{\text{LO}}(\mathbf{v}, 0) = (\pi\sigma_{\text{LO}}^2)^{-1/2} \exp\left(-\frac{v^2}{2\sigma_{\text{LO}}^2} - \frac{ikv^2}{2F_{\text{LO}}}\right), \tag{185}$$

where σ_{LO} (m) is the $1/e$ intensity radius of the beam, and F_{LO} (m) is the phase curvature of the beam. (Positive F_{LO} indicates a beam waist on the detector side of the receiver.) The normalized field of the BPLO is

$$e_{\text{BPLO}}(\mathbf{v}, 0) = (\pi\sigma_{\text{LO}}^2)^{-1/2} \exp\left(-\frac{v^2}{2\sigma_{\text{RE}}^2} - \frac{ikv^2}{2F_{\text{RE}}}\right), \tag{186}$$

where

$$\frac{1}{\sigma_{\text{RE}}^2} = \frac{1}{\sigma_R^2} + \frac{1}{\sigma_{\text{LO}}^2}, \tag{187}$$

$$\frac{1}{F_{\text{RE}}} = \frac{1}{F_R} - \frac{1}{F_{\text{LO}}}. \tag{188}$$

The leading term of the lf series for coherent responsivity is [using Eqs. (135) and (178)]

$$C_0^{\text{lf}}(R) = \frac{\pi\sigma_{\text{TE}}^2\sigma_{\text{RE}}^2}{\sigma_L^2 R^2}\left[\frac{1}{4} + \frac{\sigma_{\text{LO}}^2}{4\sigma_R^2} + \frac{\sigma_{\text{LO}}^2}{4\sigma_{\text{TE}}^2} + \left(1 - \frac{R}{F_{\text{TE}}}\right)^2 \frac{k^2\sigma_{\text{TE}}^2\sigma_{\text{LO}}^2}{4R^2} + \left(1 - \frac{R}{F_{\text{RE}}}\right)^2 \frac{k^2\sigma_{\text{RE}}^2\sigma_{\text{LO}}^2}{4R^2} + \frac{\sigma_{\text{LO}}^2}{\rho_0^2(R)}\right]^{-1}, \tag{189}$$

and the leading-order expression for heterodyne efficiency is [using Eqs. (84), (167), and (189)]

$$\eta_{H_0}^{\text{lf}}(R) = \frac{\sigma_{\text{RE}}^2}{\sigma_R^2}\left[\frac{1}{4} + \frac{\sigma_{\text{LO}}^2}{4\sigma_R^2} + \frac{\sigma_{\text{LO}}^2}{4\sigma_{\text{TE}}^2} + \left(1 - \frac{R}{F_{\text{TE}}}\right)^2 \frac{k^2\sigma_{\text{TE}}^2\sigma_{\text{LO}}^2}{4R^2} + \left(1 - \frac{R}{F_{\text{RE}}}\right)^2 \frac{k^2\sigma_{\text{RE}}^2\sigma_{\text{LO}}^2}{4R^2} + \frac{\sigma_{\text{LO}}^2}{\rho_0^2(R)}\right]^{-1}. \tag{190}$$

The SNR is given by Eqs. (79) and (89) for uniform diffuse and aerosol targets, respectively. The assumptions employed in deriving these results are listed in Table I.

Equations (189) and (190) describe the loss of the SNR and heterodyne efficiency caused by several physical mechanisms of monostatic CLR. The second term in the brackets in the denominator contains the mismatch between the LO and backscattered beam profile on the detector. The third and fourth terms represent the loss of received field coherence caused by the incoherent aerosol target in the absence of refractive turbulence. The third term is the diffraction component of the transmitted beam, and the fourth term is the corresponding geometrical optics component. The fifth term is the mismatch between the phase-front curvature of the LO field and the total backscattered field as modified by the receiver. The last term is the effect of atmospheric refractive turbulence, which includes two mechanisms: the first mechanism is the expansion of the transmitted beam caused by refractive turbulence, which produces a larger incoherent image at the target, and the second mechanism is the loss of coherence of the backscat-

Table I. Assumptions for Calculations

(1) Monostatic heterodyne detection laser radar system
(2) Small fractional frequency difference between transmitter and LO
(3) Transmitted pulse profile changes slowly compared with optical period
(4) Untruncated Gaussian transmitted beam
(5) Untruncated Gaussian transmitter/receiver lens
(6) Untruncated Gaussian LO
(7) Ideal polarization match
(8) Ideal square-law detector for i.f. power
(9) Uniform quantum efficiency across the photovoltaic detector
(10) Large detector area compared with LO size
(11) Shot-noise-limited heterodyne detection
(12) Received power much smaller than LO power
(13) Locally stationary atmosphere
(14) Kolmogorov refractive-turbulence spectrum
(15) Weak integrated refractive turbulence
(16) Square-law structure function ($x^{5/3} \to x^2$) on the leading term of path-integral expansion
(17) Paraxial approximation or Fresnel diffraction theory
(18) Markov approximation (turbulence in statistically independent layers)
(19) Backscatter coefficient β is a function of range only
(20) No optical aberrations or misalignments
(21) Independent refractive turbulence on forward and backward paths
(22) Extinction the same for transmit and backscatter paths

tered field as it propagates through the refractive turbulence.

The symmetric representation of coherent responsivity is

$$C_0^{\mathrm{lf}}(R) = \frac{\pi\sigma_{\mathrm{TE}}^2\sigma_{\mathrm{RE}}^2}{\sigma_L^2\sigma_{\mathrm{LO}}^2R^2}\left[\frac{1}{4\sigma_{\mathrm{RE}}^2} + \frac{1}{4\sigma_{\mathrm{TE}}^2} + \left(1 - \frac{R}{F_{\mathrm{TE}}}\right)^2\frac{k^2\sigma_{\mathrm{TE}}^2}{4R^2} + \left(1 - \frac{R}{F_{\mathrm{RE}}}\right)^2\frac{k^2\sigma_{\mathrm{RE}}^2}{4R^2} + \frac{1}{\rho_0^2(R)}\right]^{-1}. \quad (191)$$

The analogous calculation in the target plane is given by Eq. (141). The average of the normalized BPLO irradiance in the target plane is

$$\langle j_{\mathrm{BPLO}}(\mathbf{p}, R)\rangle = \frac{\sigma_{\mathrm{RE}}^2}{\pi\sigma_{\mathrm{LO}}^2\sigma_{\mathrm{BR}}^2(R)}\exp\left(-\frac{p^2}{\sigma_{\mathrm{BR}}^2(R)}\right), \quad (192)$$

where

$$\sigma_{\mathrm{BR}}^2(R) = \sigma_{\mathrm{RE}}^2(1 - R/F_{\mathrm{RE}})^2 + \frac{R^2}{k^2\sigma_{\mathrm{RE}}^2} + \frac{2R^2}{k^2\rho_0^2(R)}, \quad (193)$$

and σ_{BR} (m) is the $1/e$ intensity radius of the imagined BPLO in the target plane. The transmitter and reciprocal receiver truncation ratios are [see Eqs. (70) and (71)]

$$T_T = \frac{\sigma_{\mathrm{TE}}^2}{\sigma_L^2}, \qquad T_R = \frac{\sigma_{\mathrm{RE}}^2}{\sigma_{\mathrm{LO}}^2}. \quad (194)$$

The coherent responsivity density in the target plane representation becomes

$$c_0^{\mathrm{lf}}(\mathbf{p}, R) = \frac{\lambda^2T_TT_R}{\pi^2\sigma_{\mathrm{BT}}^2(R)\sigma_{\mathrm{BR}}^2(R)}\exp\left(-\frac{p^2}{\sigma_{\mathrm{BT}}^2(R)} - \frac{p^2}{\sigma_{\mathrm{BR}}^2(R)}\right). \quad (195)$$

Performing the integration over the target coordinate [Eq. (80)] produces

$$C_0^{\mathrm{lf}}(R) = \frac{\lambda^2T_TT_R}{\pi[\sigma_{\mathrm{BT}}^2(R) + \sigma_{\mathrm{BR}}^2(R)]}, \quad (196)$$

which is equivalent to Eq. (189). Note that the radius of the LO, σ_{LO}, appears as a separate parameter and that CLR SNR cannot be specified by only σ_{TE}, F_{TE}, σ_{RE}, F_{RE}, and ρ_0. For fixed transmitter power P_T, atmospheric parameters $[\beta(R), K(R)]$, and receiver parameters $(\sigma_{\mathrm{RE}}, F_{\mathrm{RE}})$, the maximum SNR occurs when $\sigma_{\mathrm{BT}} \ll \sigma_{\mathrm{BR}}$; i.e., the size of the transmitted beam on the target is much less than the size of the imagined BPLO on the target, or equivalently, the transmitter dimensions are much larger than the receiver dimensions. This condition was noted by Fluckiger *et al.*[89] in the far-field limit and is shown here to be generally true. Note that this is not a practical case because the transmitter dimensions are much larger than the receiver dimensions and the cost performance is poor.

1. *Fixed Receiver Lens*

For a given receiver lens (fixed σ_R and F_R) the maximum heterodyne efficiency occurs when the field accepted by the receiver matches the LO field. This occurs when all the mechanisms for the loss of heterodyne efficiency in Eq. (189) are negligible. The effects of atmospheric refractive turbulence are removed when $\rho_0(R) \gg \sigma_{\mathrm{LO}}$ $(C_n^2 \to 0)$. The loss of heterodyne efficiency from the geometrical component of the illuminated target is removed when $F_{\mathrm{TE}} = R$. The loss of heterodyne efficiency from the diffraction component of the illuminated target is removed when $\sigma_{\mathrm{TE}} \gg \sigma_{\mathrm{LO}}$; i.e., a compact illuminated image is produced at the target that approximates a point source and produces a coherent spherical wave over the dimensions of the LO at the receiver. The phase front of the received field is matched to the phase front of the LO when $F_{\mathrm{RE}} = R$. These limits produce a coherent field incident on the receiver. The receiver lens converts this coherent field into a coherent Gaussian field of the proper phase curvature, which is mixed with the Gaussian LO field. The spatial distributions of these two fields are matched when $\sigma_{\mathrm{LO}} = \sigma_R$ $(\sigma_{\mathrm{RE}}^2 = \sigma_R^2/2)$. Then the heterodyne efficiency, Eq. (190), is unity and [see Eq. (84)]

$$C_0^{\mathrm{lf}}(R) = D_0^{\mathrm{lf}}(R), \quad (197)$$

and the coherent detection responsivity is equal to the direct detection responsivity. Note that the condition for maximum heterodyne efficiency is not a feasible geometry since the transmitter is much larger than the receiver dimensions. Therefore practical CLR's will always have a maximum heterodyne efficiency and maximum system efficiency that are less than unity.

The receiver plane (detector plane) calculation provides a clear connection to the physics of CLR. The corresponding interpretation in the target plane is not as clear. The overlap integral for the case of unity heterodyne efficiency corresponds to a small transmitted beam size on the target compared with the BPLO beam size, and with reciprocal receiver parameters chosen to give maximum irradiance over the overlap region. Note that matching the two irradiance profiles in the target plane does not produce maximum heterodyne efficiency but produces maximum coherent responsivity when there is no refractive turbulence.[90]

2. *Optimal LO Parameters*

For a given transmitter and receiver geometry (fixed σ_{TE}, F_{TE}, σ_R, and F_R) and a target at range R, the optimal LO parameters for maximum SNR, maximum heterodyne efficiency η_H, and maximum system efficiency η_S are

$$\sigma_{\mathrm{LO}}^{\mathrm{opt}} = \sigma_R\left[1 + \frac{k^2}{R^2}\sigma_R^2\sigma_{BT}^2(R) + 2\frac{\sigma_R^2}{\rho_0^2(R)}\right]^{-1/4}, \quad (198)$$

$$F_{\mathrm{LO}}^{\mathrm{opt}} = \frac{RF_R}{R - F_R}, \quad (199)$$

which produces maximum performance at the range $R = F_{\mathrm{TE}}$. These optimum LO values usually are not

implemented in real CLR systems because they depend on the target range R.

3. Optimal Conditions for a Gaussian Monostatic CLR System

The maximum SNR for a uniform diffuse target is obtained by maximizing coherent responsivity. The governing equations for maximum SNR for the monostatic CLR have been derived[90] by using functional maximization, and analytic solutions have been obtained for the Gaussian aperture CLR system. For a monostatic CLR the transmitter lens and receiver lens are the same [$W_T(\mathbf{u}) = W_R(\mathbf{u})$]. Then $\sigma_T = \sigma_R$ and $F_T = F_R$. We now determine the conditions for maximum SNR and coherent responsivity for a given range R and fixed receiver and transmitter lens dimension σ_R. This requires that $\rho_0(R) \rightarrow \infty$ (no refractive turbulence), $F_{TE} = R$, and $F_{RE} = R$. Taking the partial derivatives of coherent responsivity (or SNR) with respect to σ_L and σ_{LO} and solving the simultaneous equations result in $\sigma_L = \sigma_{LO} = \sigma_R/\sqrt{2} = 0.707\sigma_R$. For the maximum SNR of this general Gaussian aperture CLR system, the heterodyne efficiency η_H is 4/9, the transmitter power truncation ratio T_T is 2/3, and the system efficiency $\eta_S(R)$ is 8/27 = 0.296 [see Eqs. (189), (190), and (194)]. Because of diffraction the transmitter cannot produce an illuminated target spot that is small enough to approximate a point source, and the received field from the target deviates from a spherical wave over the effective area of the receiver. These results agree with the results from functional maximization.[90] The optimal performance of a CLR system with a more realistic circular transmitter–receiver aperture of radius R_A and Gaussian laser and LO field was considered by Rye,[23] Wang,[32] and Zhao *et al.*[33] This laser radar has the same collecting area A_R as the Gaussian aperture system when $R_A = \sigma_R$. The optimal parameters for the circular aperture with the same collecting area and a Gaussian LO incident on the detector are $\sigma_L = \sigma_{LO} = R_A/1.763 = 0.5672R_A$, which is close to the condition for the Gaussian aperture system. However, the system efficiency η_S for the circular aperture system is 0.40118, which is a factor of 1.354 better than the Gaussian aperture system. Rye[23] obtained a system efficiency of 0.43837 for the Gaussian monostatic lidar with a circular aperture by using an improved LO design. A monostatic circular aperture CLR has a better SNR than a comparable untruncated Gaussian aperture CLR system with an equal collecting area. (Other noncircular apertures may have a higher SNR than a circular aperture with an equal collecting area.)

The maximum SNR, heterodyne efficiency, and coherent responsivity for the general Gaussian CLR system require a focused condition ($R = F_{TE} = F_{RE} = F$) or, equivalently, the far-field condition. With parameters optimized ($\sigma_L = \sigma_{LO} = \sigma_R/\sqrt{2}$) for this focused condition, the heterodyne efficiency at any range R becomes

$$\eta_H(R) = \frac{4}{9}\left[1 + \left(1 - \frac{R}{F}\right)^2 \frac{k^2\sigma_R^4}{9R^2} + \frac{2}{3}\frac{\sigma_R^2}{\rho_0^2(R)}\right]^{-1}. \tag{200}$$

The behavior of this heterodyne efficiency and SNR for a typical CLR is presented in Section VI. Using the optimal parameters for the general Gaussian CLR system provides useful analytic expressions for studying CLR performance.

4. Receiver Lens Larger than the LO Beam

When the dimension of the receiver lens σ_R is much larger than the dimension of the LO beam σ_{LO} (i.e., negligible receiver truncation of the LO), then $\sigma_{RE} = \sigma_{LO}$, and Eq. (189) becomes

$$C_0^{lf}(R) = \frac{\pi\sigma_{LO}^2}{\left[\frac{1}{4} + \frac{\sigma_{LO}^2}{4\sigma_{TE}^2} + \left(1 - \frac{R}{F_{TE}}\right)^2 \frac{k^2\sigma_{TE}^2\sigma_{LO}^2}{4R^2} + \left(1 - \frac{R}{F_{RE}}\right)^2 \frac{k^2\sigma_{LO}^4}{4R^2} + \frac{\sigma_{LO}^2}{\rho_0^2(R)}\right]R^2}. \tag{201}$$

The effective receiver aperture is defined by the LO, and the SNR is independent of the parameter σ_R; however, the heterodyne efficiency is poor since much of the backscattered field does not mix with the LO field. This was noted by Wang[29] for the case of a Gaussian LO and a circular aperture. This limit ($\sigma_R \rightarrow \infty$) has been used by many authors (see Section V) and is the correct limit if the physical receiver mirror is sufficiently larger than the BPLO beam. If we further assume a matched monostatic CLR system, $F_{TE} = F_{RE} = F$ and $\sigma_{TE} = \sigma_{LO} = \sigma$, assume a short pulse duration, substitute $D_2 = 2\sqrt{2}\sigma$ ($1/e^2$ intensity diameter) and $B = 1/\tau$, where τ (s) is the pulse duration (matched filter assumption), and utilize Eqs. (92) and (201), the SNR becomes

$$\mathrm{SNR} = \frac{\pi\eta_Q U_T \beta c\tau D_2^2 [K(R)]^2}{8h\nu R^2\left[1 + \left(\frac{D_2}{2\rho_0}\right)^2 + \left(\frac{\pi D_2^2}{4\lambda R}\right)^2\left(1 - \frac{R}{F}\right)^2\right]}, \tag{202}$$

which is a commonly used form of the CLR equation.[6] Further simplification occurs if we assume negligible refractive-turbulence effects ($\rho_0 \gg D_2$) and either focused ($R = F$) or far-field operation ($D_2^2/\lambda \ll R < F$):

$$\mathrm{SNR} = \frac{\pi\eta_Q U_T \lambda\beta D_2^2 [K(R)]^2}{8hBR^2}, \tag{203}$$

which is often used for the CLR equation, especially for space-based systems.[91]

B. High-Spatial-Frequency Calculation

The leading-order term for the hf behavior of the mutual coherence of the normalized backscattered field at the receiver plane is given by[48] [use Eqs. (133), (134), (136), (149), and (160) and the square-law structure function approximation]

$$m_{S_0}^{\mathrm{hf}}(\mathbf{v}_1, \mathbf{v}_2, 0) = \frac{T_T}{R^2[1 + \sigma_{TE}^2/\rho_0^2(R)]} \times \exp\left\{\frac{ik}{R}[1 - (1 - R/F_{TE})/[1 + \rho_0^2(R)/\sigma_{TE}^2]]\mathbf{r}\cdot\mathbf{s} - \frac{s^2\sigma_{TE}^2k^2(1 - R/F_{TE})^2}{4R^2[1 + \sigma_{TE}^2/\rho_0^2(R)]} - \frac{s^2}{4\sigma_{TE}^2} - \frac{r^2}{\sigma_{TE}^2 + \rho_0^2(R)}\right\}. \quad (204)$$

The normalized backscattered irradiance is given by

$$m_{S_0}^{\mathrm{hf}}(\mathbf{v}, \mathbf{v}, 0) = \frac{T_T}{R^2[1 + \sigma_{TE}^2/\rho_0^2(R)]}\exp\left[-\frac{v^2}{\sigma_{TE}^2 + \rho_0^2(R)}\right], \quad (205)$$

which can be written as

$$m_{S_0}^{\mathrm{hf}}(\mathbf{v}, \mathbf{v}, 0) = \frac{m_{S_0}^{\mathrm{lf}}(\mathbf{v}, \mathbf{v}, 0)}{[1 + \sigma_{TE}^2/\rho_0^2(R)]}\exp\left[-\frac{v^2}{\sigma_{TE}^2 + \rho_0^2(R)}\right]. \quad (206)$$

When the field coherence length is larger than the effective transmitter beam dimensions [$\rho_0(R) \gg \sigma_{TE}$], the average irradiance of the backscattered field from the leading-order term of the hf series has a maximum enhancement at the transmitter axis ($\mathbf{v} = 0$) equal to the free-space irradiance [$m_{S_0}^{\mathrm{lf}}(\mathbf{v}, \mathbf{v}, 0)$], and the transverse scale of this enhancement is the field coherence length. For the more common case of small-field coherence length compared to the effective transmitter beam dimensions [$\rho_0(R) \ll \sigma_{TE}$], the magnitude of the enhancement is reduced, and the transverse scale becomes the effective transmitter dimensions σ_{TE}.

The complex degree of coherence for the leading term of the hf behavior is

$$\hat{m}_{S_0}^{\mathrm{hf}}(\mathbf{v}_1, \mathbf{v}_2, 0) = \exp\left\{\frac{ik}{R}\mathbf{r}\cdot\mathbf{s}[1 - (1 - R/F_{TE})/[1 + \rho_0^2(R)/\sigma_{TE}^2]] - \frac{s^2}{2\hat{\rho}_0^2(R)}\right\}, \quad (207)$$

where

$$\frac{1}{\hat{\rho}_0^2(R)} = \frac{k^2}{2R^2[1 + \sigma_{TE}^2/\rho_0^2(R)]}\left[\sigma_{TE}^2(1 - R/F_{TE})^2 + \frac{R^2}{k^2\sigma_{TE}^2}\right], \quad (208)$$

and $\hat{\rho}_0(R)$ is the field coherence length of the backscattered field at the axis of the transmitter beam.

The coherent responsivity becomes

$$C_0^{\mathrm{hf}}(R) = \frac{\pi T_T T_R}{R^2}\left\{\frac{k^2}{4R^2}[\sigma_{BT}^2(R) + \sigma_{BR}^2(R)] + \frac{1}{4\rho_0^2(R)} \times \left[\frac{\sigma_{RE}^2}{\sigma_{TE}^2} + \frac{\sigma_{TE}^2}{\sigma_{RE}^2} + k^2\sigma_{TE}^2\sigma_{RE}^2(F_{TE}^{-1} - F_{RE}^{-1})^2 - 2\right]\right\}^{-1}. \quad (209)$$

When we use Eqs. (149) and (160) and the square-law-structure function limit, the coherent responsivity density is

$$c_0^{\mathrm{hf}}(\mathbf{p}, R) = \frac{\lambda^2 T_T T_R}{\pi^2\sigma_0^2(R)\sigma_1^2(R)}\exp[-p^2/\sigma_0^2(R)], \quad (210)$$

where

$$\sigma_1^2(R) = \sigma_{BT}^2(R) + \sigma_{BR}^2(R) + R_S^2(R)\left[\frac{\sigma_{RE}^2}{\sigma_{TE}^2} + \frac{\sigma_{TE}^2}{\sigma_{RE}^2} + k^2\sigma_{TE}^2\sigma_{RE}^2(F_{TE}^{-1} - F_{RE}^{-1})^2 - 2\right], \quad (211)$$

$$\sigma_0^2(R) = R_S^2(R) + [R_S^2(R)[\sigma_{BT}^2(R) + \sigma_{BR}^2(R)] + \sigma_{BT}^2(R)\sigma_{BR}^2(R)]\sigma_1^{-2}. \quad (212)$$

The correlation of the small-scale fluctuations of transmitted and imagined BPLO irradiance at the target has a Gaussian profile with a width σ_0 (m).

The coherent responsivity is obtained by integrating Eq. (210) over p, i.e.,

$$C_0^{\mathrm{hf}}(R) = \frac{\lambda^2 T_T T_R}{\pi\sigma_1^2(R)}, \quad (213)$$

which agrees with the receiver plane calculation, Eq. (209).

The leading-order term for the hf behavior of the direct responsivity is [use Eqs. (83), (151), (160) and the square-law structure function approximation]

$$D_0^{\mathrm{hf}}(R) = \frac{T_T\Omega(R)\rho_0^2(R)}{[\rho_0^2(R) + \sigma_{TE}^2 + \sigma_R^2]}. \quad (214)$$

When $R_F > \rho_0(R) \gg \sigma_{TE}$ and σ_R,

$$D_0^{\mathrm{hf}}(R) = T_T\Omega(R) = D_0^{\mathrm{lf}}(R). \quad (215)$$

The backscatter intensity enhancement from the leading-order term of the hf behavior is equal to the backscatter irradiance at the receiver with no refractive turbulence. This increase in direct detection power produces a factor of 2 increase in the SNR (heterodyne efficiency does not change) compared to the statistically independent-path calculation for large path-integrated refractive turbulence. The phase approximation of the extended Huygens–Fresnel theory does not predict this effect.[20] When $R_F > \rho_0(R) \gg \sigma_{TE}$ and σ_R, $N_0 \ll 1$ in Fig. 1 of Ref. 20. The calculation using the phase approximation of the extended Huygens–Fresnel theory is equal to the statistically independent-path calculation.

When $\rho_0(R) < R_F \ll \sigma_{TE}$ and σ_R,

$$D_0^{\mathrm{hf}}(R) = \frac{D_0^{\mathrm{lf}}(R)\rho_0^2(R)}{\sigma_{TE}^2 + \sigma_R^2}. \quad (216)$$

The backscatter intensity enhancement from the hf component integrated over the receiver aperture [$D_0^{\mathrm{hf}}(R)$] is small compared with the contribution from the lf component [$D_0^{\mathrm{lf}}(R)$]. For the matched

monostatic CLR [$e_T(\mathbf{u}, 0) = e_{BPLO}(\mathbf{v}, 0)$] and large path-integrated refractive turbulence, the SNR is twice the statistically independent-path calculation [see Eq. (148)]. This behavior is predicted by the phase approximation of the extended Huygens–Fresnel theory.[20] When $\rho_0(R) \ll \sigma_{TE}$ and σ_R the increase in the SNR is due to an increase in heterodyne efficiency from the hf component (see Fig. 4). The direct detection power is unchanged.

V. Comparison with Previous Results

There have been several results published for monostatic CLR systems with Gaussian geometries. We now compare our results with these previous works.

Sonnenschein and Horrigan[12] calculated the SNR for a monostatic CLR with Gaussian transmitter, receiver, and LO but neglected refractive turbulence. The conversion of notation is $\eta_Q \to \eta$, $\sigma_{TE}^2 = \sigma_{LO}^2 \to R^2/2$, $F_{TE} = F_{RE} \to f$, $R \to L$, $\rho_0(R) = \sigma_R = F_{LO} \to \infty$, $K(R) \to 1$, $\beta(R) \to \beta(\pi)$, and $k \to 2\pi/\lambda$. The noise power was specified as that from a photoconductive detector, but a photovoltaic expression was used. Then our Eq. (89) with Eq. (189) becomes

$$\mathrm{SNR} = \frac{\eta P_T \beta(\pi) \pi R^2}{h\nu B} \int_0^\infty \frac{dL}{\left[1 + \left(\frac{\pi R^2}{\lambda L}\right)^2 \left(1 - \frac{L}{f}\right)^2\right] L^2}, \quad (217)$$

which matches their Eq. (20) except for a factor of 2. The factor of 2 error is traced to their Eq. (13), where a factor of $\sqrt{2}$ is omitted. However, since photoconductive noise power is a factor of 2 larger than photovoltaic noise, their final results are correct for the specified case of photoconductive noise, since the two factors of 2 cancel.

Yura[15] calculated the CLR SNR reduction factor ψ caused by refractive turbulence for a Gaussian transmitter and Gaussian LO but ignored the receiver lens. The conversion of notation is $\sigma_{TE} \to a$, $F_{TE} \to f$, $\sigma_{LO} \to b$, $R \to z$, $\rho_0(R) \to \rho_R$, $\sigma_R = F_{RE} \to \infty$ ($\sigma_{RE} \to b$), and $\psi \to \eta_H/\eta_H[\rho_0(R) = \infty]$ [see Eq. (190)]. Then ψ becomes

$$\psi = \frac{b^2 + a^2[1 - (z/f)]^2 + (z/ka)^2 + (z/kb)^2}{b^2 + a^2[1 - (z/f)]^2 + (z/ka)^2 + (z/kb)^2 + (2z/k\rho_R)^2}, \quad (218)$$

which should match Yura's Eq. (41). The b^2 terms in the numerator and denominator are missing from Eq. (41) of Yura because the phase curvature term $(ik/2z)(p_1^2 - p_2^2)$ of his Eq. (23) was dropped in going to his Eq. (25). This is equivalent to the far-field assumption.

Clifford and Wandzura[20] calculated the CLR power reduction (no detector noise was considered) including the refractive turbulence for the identical Gaussian transmitter and combined receiver LO. Their result [Eq. (15)] for propagation through statistically independent atmospheric paths is proportional to our result [Eqs. (92) and (189)] with the conversion of notation $\sigma_{TE} = \sigma_{RE} \to D_0/2$, $F_{TE} = F_{RE} \to f$, $R \to z$, and $\rho_0^2(R) \to \rho_0^2/2$.

Wang[22] calculated the average CLR power (no detector noise was considered) for a diffuse target, uncorrelated atmospheric turbulence, no receiver lens, and LO matched to the transmitter. His Eq. (47) is proportional to our Eq. (92) with Eq. (189) under the conversion of notation $\sigma_R = F_R \to \infty$, $\sigma_{TE} = \sigma_{LO} \to \alpha_0$, $\sigma_{RE} \to \alpha_0$, $F_{TE} \to F_0$, $F_{LO} \to -F_0$, $F_{RE} \to F_{LO}$, $6.88\,\rho_0^2 \to r_0^2$, and $R \to L$. These linkages to prior work support the validity of our general results.

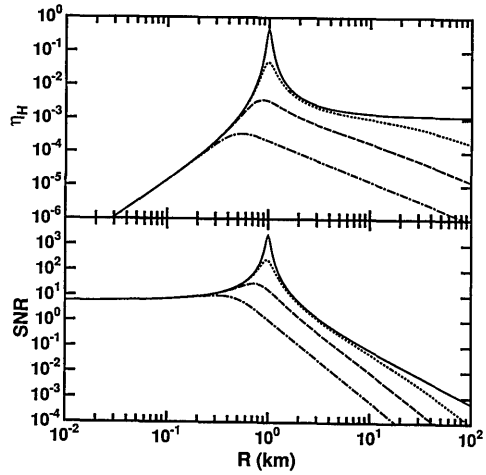

Fig. 3. Heterodyne efficiency η_H and the SNR as a function of range R by using the statistically independent-path calculation for a monostatic laser radar system [see Eqs. (92), (189), and (190)] at a wavelength of 1.064-1 μm and focused at 1 km ($F_{TE} = F_{RE} = F = 1$ km). The system parameters are $\sigma_R = 10.0$ cm, $\sigma_L = \sigma_{LO} = 7.07$ cm, $F_{LO} = \infty$, $U_T = 5$ mJ, $\beta(R) = \beta = 4 \times 10^{-6}\,\mathrm{m^{-1}\,sr^{-1}}$, $K(R) = 1.0$, $\eta_Q = 0.5$, and $B = 50$ MHz. The level of refractive turbulence C_n^2 has the values $C_n^2 = 0$ (—), $C_n^2 = 10^{-14}\,\mathrm{m^{-2/3}}$ (· · ·), $C_n^2 = 10^{-13}\,\mathrm{m^{-2/3}}$ (- - - -), $C_n^2 = 10^{-12}\,\mathrm{m^{-2/3}}$ (· - · -).

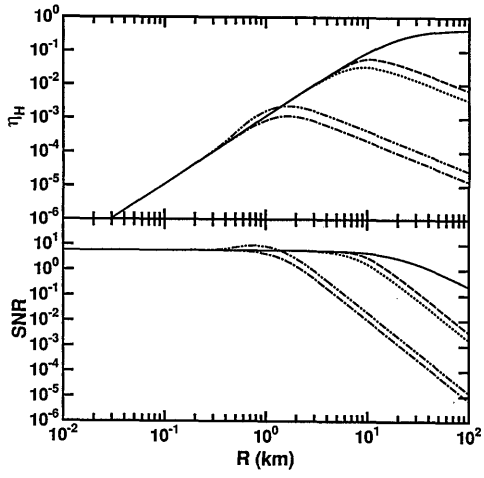

Fig. 4. Heterodyne efficiency η_H and the SNR as a function of range R for a collimated Gaussian monostatic laser radar system at a wavelength of 1.064 μm. The system parameters are $F_{TE} = F_{RE} = \infty$, $\sigma_R = 10.0$ cm, $\sigma_L = \sigma_{LO} = 7.07$ cm, $F_{LO} = \infty$, $U_T = 5$ mJ, $\beta = 4 \times 10^{-6}\,\mathrm{m^{-1}\,sr^{-1}}$, $K(R) = 1.0$, $\eta_Q = 0.5$, and $B = 50$ MHz. The level of refractive turbulence C_n^2 has the values of $C_n^2 = 0$ (—); $C_n^2 = 10^{-15}\,\mathrm{m^{-2/3}}$, lf calculation [see Eqs. (84), (92), (167), and (200)] (· · ·), lf plus hf calculation [see Eqs. (84), (92), (167), (169), (170), (189), (209), and (214)] (- - - -); and $C_n^2 = 10^{-13}\,\mathrm{m^{-2/3}}$, lf calculation (· - · -), lf plus hf calculation (·· - ·· -).

Table II. Diversification of Coherent Laser Radar Theory

Detector:	Large uniform η_Q	Finite uniform η_Q	Variable η_Q
Target:	Glint	Aerosol	Diffuse
	Mirror	Retroreflector	General
Geometry:	Monostatic	Bistatic	
Analysis plane:	Detector	Receiver	Target
Power normalization:	Laser power	Transmitter power	Noise power
Propagation regimes:	Near field	Near field focused	Far field
Transmitter/receiver:	Untruncated Gaussian	Circular	General aperture
Laser/LO field:	Gaussian	Gaussian modes	General
Refractive turbulence:	Spectrum	Turbulence profile	Intermittency
Theoretical method:	Rhytov	Extended Huygens–Fresnel	Path integral
	Functional methods	Two-scale expansion	Heuristic
Scintillation regimes:	Low spatial frequencies	High spatial frequencies	
Performance criterion:	SNR	Heterodyne efficiency	Coherent responsivity
	System efficiency	Coherent receiver area	

VI. Calculations

The conditions for the optimal performance of a general Gaussian CLR system were determined in Subsection IV.A. The behavior of the SNR and heterodyne efficiency for the lf behavior as a function of range and level of refractive turbulence C_n^2 for a typical focused CLR system[38] with optimal parameters [Eqs. (84), (92), (167), and (200)] is shown in Fig. 3. Here $\lambda = 1.0641$ μm, $\sigma_R = 10.0$ cm, $\sigma_L = \sigma_{LO} = 7.07$ cm, $F_{TE} = F_{RE} = F = 1$ km, $U_T = 5$ mJ, and refractive turbulence strength C_n^2 is assumed uniform with range. As expected, the best performance is obtained at the focal distance with small C_n^2. The collimated case $F_{TE} = F_{RE} = F = \infty$ and the lf and hf calculations [Eqs. (92) and (84) using Eqs. (169) and (170)] are shown in Fig. 4. The near-field behavior is important for all ranges of <10 km. The enhancement of the SNR at large distances is due to an enhancement in heterodyne efficiency from the hf contribution. Note the region of superenhancement (a SNR higher than predicted for no refractive turbulence; see Subsection III.A) near the 1-km range.

VII. Conclusions and Recommendations

The use of shorter wavelengths in CLR systems makes the theoretical treatment of atmospheric refractive turbulence and near-field, nonfocused conditions more important. The analytic expressions derived here are complementary to numerical investigations and lead to an insight and understanding of CLR physics, operating regimes, parameter dependencies, and optimizations.

The numerous choices or branches possible when considering CLR theory present a formidable multidimensional parameter space, as Table II conveys. We chose notation and normalization to provide the clearest extension of previous results to the most general conditions.

The performance of CLR can be determined by calculations of the SNR [Eq. (14)] and heterodyne efficiency [Eq. (15)]. The SNR is proportional to the product of two terms [Eq. (17)]: the direct detection power $P_D(t)$ and the heterodyne efficiency η_H. The heterodyne efficiency can be estimated from the laser radar signal for general conditions. These expressions are defined by the fields in the detector plane. The SNR and heterodyne efficiency can also be calculated in the receiver plane (Subsection II.B) and the target plane (Subsection II.C). It is essential to perform calculations in both the target plane and the receiver plane to understand fully the physics of CLR performance, especially when refractive turbulence is important. For a large detector with uniform quantum efficiency and for many common targets, the SNR can be expressed in terms of the target characteristics and in terms of the coherent responsivity (Subsection II.D), which contains all the system and atmospheric refractive turbulence contributions to the SNR. The coherent responsivity is related to the heterodyne efficiency and the direct responsivity, which contains all the system and atmospheric refractive turbulence contributions to direct detection power. The results for a large detector with uniform quantum efficiency are extended to the case of a finite detector with uniform quantum efficiency (Subsection II.G) and a detector with varying quantum efficiency (Subsection II.H). The results for aerosol targets are directly related to the results for diffuse hard targets; thus calibration methods based on hard targets are justified.

The effects of atmospheric refractive turbulence (Section III) are included by using path-integral expansions that produce two separate series, the lf series and the hf series. The lf series describes the contribution to system performance from the large-scale scintillation processes. When the intensity fluctuations on the target are small, the first term of the lf series yields the dominant behavior. This term is equivalent to the assumption of statistically independent paths and simplifies the numerical calculations for a number of problems, in particular, monostatic CLR calculations for short propagation paths. The enhancement of the SNR over the statistically independent path calculation is only possible if the irradiance fluctuations on the target are appreciable. In this region the small-scale scintillation appears on the target and the hf series becomes important. In the limit of large path-integrated refractive turbulence,

the SNR approaches twice the statistically independent path calculation when the transmitted and BPLO fields are matched. The enhancement of the SNR compared to no refractive turbulence (super enhancement) is also possible for a variety of parameter regimes.

The effects of the different physical mechanisms on CLR performance were determined by calculations of the SNR and heterodyne efficiency for untruncated Gaussian transmitter, receiver, and LO (Section IV) for the leading-order term of both the lf and hf series. A heterodyne efficiency of unity is possible when the dimensions of the transmitter are much larger than the dimensions of the receiver. However, this is not a practical system, and heterodyne efficiency is less than unity for the more useful monostatic configuration. The SNR and heterodyne efficiency for the optimal Gaussian laser radar system are shown for a typical 1.0641-μm wavelength system (Figs. 3 and 4) and demonstrate that the near-field region and atmospheric refractive turbulence are more important than for 10.6-μm wavelength systems.

Extensions of this work include the CLR SNR, system efficiency η_S, and heterodyne efficiency η_H theory and calculations appropriate for

(1) arbitrary transmitter, receiver, LO, and detector response;
(2) medium and strong path-integrated refractive- turbulence conditions;
(3) the use of optical fibers for mixing fields;
(4) general scattering surfaces;
(5) bistatic CLR systems in strong path-integrated refractive turbulence;
(6) space–time statistics of real atmospheric refractive turbulence;
(7) refractive-turbulence spectra for real atmospheric conditions;
(8) effects of misalignments; and
(9) effects of optical aberrations.

Many of these theoretical extensions may be analytically intractable, and numerical calculations and simulations may be required. However, because of the difficulty of performing numerical calculations that include the effects of refractive turbulence, analytical expressions based on expansions for the transmitter field, receiver lens, and LO field would be useful for understanding laser radar performance. They also provide benchmarks for testing the accuracy of any numerical calculation.

Appendix A: Average Intermediate Frequency Heterodyne Power

Using the complex representation of a real expression, Eq. (8) becomes

$$i_S(t) = \frac{G_D e}{h\nu} \int_D \eta_Q(\mathbf{w})[E_S(\mathbf{w}, L, t)E_{LO}^*(\mathbf{w}, L) \exp(i\Delta\omega t + i\theta_S) + E_S^*(\mathbf{w}, L, t)E_{LO}(\mathbf{w}, L) \exp(-i\Delta\omega t - i\theta_S)]d\mathbf{w}. \quad \text{(A1)}$$

The average CLR power is the ensemble average of the square of $i_S(t)$, i.e.,

$$\begin{aligned}\langle i_S^2(t)\rangle = \left|\frac{G_D e}{h\nu}\right|^2 \int_D \int_D \eta_Q(\mathbf{w}_1)\eta_Q(\mathbf{w}_2) \\ \times [\langle E_S(\mathbf{w}_1, L, t)E_S^*(\mathbf{w}_2, L, t)\rangle\langle E_{LO}^*(\mathbf{w}_1, L)E_{LO}(\mathbf{w}_2, L)\rangle \\ + \langle E_S(\mathbf{w}_2, L, t)E_S^*(\mathbf{w}_1, L, t)\rangle\langle E_{LO}^*(\mathbf{w}_2, L)E_{LO}(\mathbf{w}_1, L)\rangle \\ + \langle E_S(\mathbf{w}_1, L, t)E_S(\mathbf{w}_2, L, t)\rangle\langle E_{LO}^*(\mathbf{w}_1, L)E_{LO}^*(\mathbf{w}_2, L)\rangle \\ \times \exp(2i\Delta\omega t + 2i\theta_S) + \langle E_S^*(\mathbf{w}_1, L, t)E_S^*(\mathbf{w}_2, L, t)\rangle \\ \times \langle E_{LO}(\mathbf{w}_1, L)E_{LO}(\mathbf{w}_2, L)\rangle \exp(-2i\Delta\omega t - 2i\theta_S)]d\mathbf{w}_1 d\mathbf{w}_2. \end{aligned} \quad \text{(A2)}$$

The first two terms are equal, and the last two terms are zero because of the ensemble average over the random phase θ_S. This produces Eq. (11).

Appendix B: Symbols

$A_{COH,R}$ (m^2)	coherent area and area of receiver;
BPLO	backpropagated local oscillator;
B (Hz)	bandwidth of detector and amplifier;
$B(\mathbf{q}_1, \mathbf{q}_2, \mathbf{p}_1, \mathbf{p}_2)$ (m^{-4} sr^{-1})	target-scattering function;
$B_n(\mathbf{x}, z)$	correlation of refractive-index fluctuations;
$C(R, t)$	coherent responsivity;
$C_n^2(z)$ ($m^{-2/3}$)	refractive-index structure constant;
$D(R, T)$	direct responsivity;
$D'(\mathbf{x}, z)$ (m^{-1})	structure function density;
$E_{BPLO,L,LO,T,S}(\mathbf{x}, R, t)$ [$(W \cdot m^{-2})^{1/2}$]	reduced field for BPLO, laser, local oscillator, transmitter, and backscattered field;
$F_{L,LO,R,T,RE,TE}$ (m)	focal length for laser, local oscillator, receiver lens, transmitter lens, effective receiver, effective transmitter;
G_D	detector amplifier gain;
$G_A(\phi)$ (m^2)	antenna gain for effective coherent area;
$G(\mathbf{p}; \mathbf{u}, R)$ (m^{-2})	Green's function for propagation through random media;
$G^f(\mathbf{p}; \mathbf{u}, R)$	Green's function for propagation through free space;
$I(t)$ (A)	total detector current;
$I_{dc,S}$ (A)	detector direct current and backscattered signal current;
$J_{T,BPLO}(\mathbf{p}, R)$ ($W m^{-1}$)	target irradiance of transmitter and BPLO;
$K(R)$	one-way irradiance extinction;
L (m)	distance from receiver aperture to detector;
LO	local oscillator;
$M_{BPLO,LO,S,T}(\mathbf{x}_1, \mathbf{x}_2, z, t)$ ($W m^{-2}$)	mutual coherence function for BPLO, LO, backscattered, and transmitter fields;
$N(\sigma_S; \mathbf{p}, R)$ (m^{-5} sr)	number density of aerosols per unit volume per unit σ_S;
$O_{BPLO,T}(\mathbf{x}, R, t)$	autocorrelation of BPLO and transmitter field;
$P_{D,L,LO,LOD,T}$ (W)	power of direct detection, laser, LO, LO on the detector, and transmitter;
R (m)	target range;
$R_{F,S,A}$ (m)	radius of Fresnel zone, scattering caused by turbulence, and circular receiver aperture;

$T_{T,R}$	power truncation of laser by transmitter aperture and of BPLO by receiver aperture;
$U_{L,T}$ (J)	pulse energy of the laser and transmitter;
$U(R)$	strength of integrated refractive turbulence;
$V(\mathbf{q}_1, \mathbf{p}_1)$ (m^{-2} $sr^{-1/2}$)	target-scattering coefficient;
$W_{R,T}(\mathbf{x})$	field transmittance for the receiver and transmitter aperture;
$Y(\boldsymbol{\kappa})$ (m^2)	Fourier transform of detector quantum efficiency $\eta_Q(\mathbf{w})$;
c (m s^{-1})	speed of light;
$c(\mathbf{p}, R, t)$ (m^{-2})	coherent responsivity density;
$c_J(\mathbf{p}_1, \mathbf{p}_2, R, t)$ (m^{-4})	joint coherent responsivity density;
$d(\mathbf{p}, R, t)$ (m^{-2})	direct responsivity density;
$d_J(\mathbf{p}_1, \mathbf{p}_2, R, t)$ (m^{-4})	joint direct responsivity density;
$e = 1.602 \times 10^{-19}$ (C)	electronic charge;
$e_{BPLO,L,LO,T}(\mathbf{x}, R, t)$ (m^{-2})	normalized fields for BPLO, laser, LO, and transmitter fields;
$h = 6.626 \times 10^{-34}$ (J s)	Planck's constant;
$i_{N,S}(t)$ (A)	noise and signal current fluctuations;
$j_{BPLO,R,T}(\mathbf{x}, R, t)$ (m^{-2})	irradiance of normalized fields for BPLO, incoherent receiver, and transmitter;
k (rad m^{-1})	wave number of the field;
$m_{BPLO,S,T}(\mathbf{x}_1, \mathbf{x}_2, z, t)$ (m^{-2})	mutual coherence function of normalized fields for the BPLO, backscattered field, and transmitter field;
$m_{SD}(\mathbf{p}, \mathbf{x}_1, \mathbf{x}_2, z, t)$ (m^{-4})	mutual coherence function density of the normalized backscattered field;
$m_{SJ}(\mathbf{p}_1, \mathbf{p}_2, \mathbf{x}_1, \mathbf{x}_2, z, t)$ (m^{-4})	joint mutual coherence function density of the normalized backscattered field;
$n(\mathbf{x}, z)$	refractive-index fluctuations;
$\mathbf{p}, \mathbf{q}$ (m)	target transverse coordinates;
$\mathbf{r}$ (m)	centroid coordinate;
r ($sr^{-1/2}$)	reflection coefficient;
$\mathbf{s}$ (m)	difference coordinate;
t (s)	time;
$\mathbf{u}$ (m)	transmitter transverse coordinate;
$\mathbf{v}$ (m)	receiver transverse coordinate;
$\mathbf{w}$ (m)	detector transverse coordinate;
$\mathbf{x}$ (m)	general transverse coordinate;
z (m)	general propagation direction;
$\alpha(z)$ (m^{-1})	linear extinction coefficient;
β (m^{-1} sr^{-1})	aerosol backscatter coefficient;
$\delta(\mathbf{p})$ (m^{-2})	2-D vector delta function;
$\eta_{Q,H,S}$	quantum, heterodyne, and system efficiency;
θ_S	phase of backscattered field compared to the LO field;
θ_P	angle between the normal of a plane surface and the transmitter axis;
$\boldsymbol{\kappa}$ (m^{-1})	spectral spatial wave number vector;
λ (m)	wavelength of the optical field;
ν (Hz)	frequency of the optical field;
ρ (sr^{-1})	backscatter coefficient of the diffuse target;
$\rho_0(R)$ (m)	transverse field coherence length;
$\sigma_{BR,BT,L,LO,R,RE,T,TE}$ (m)	Gaussian width of the BPLO beam, transmitter beam, laser, LO, receiver lens, effective receiver, transmitter lens, effective transmitter;
σ_I^2	normalized variance of irradiance;
σ_S (m^2)	backscatter cross section for point scatterer;
τ (s)	pulse duration;
Φ (rad)	angle between target vector and propagation axis;
ω (rad s^{-1})	angular frequency of the transmitted field;
ω_{LO} (rad s^{-1})	angular frequency of the LO field;
$\Phi_n(\boldsymbol{\kappa}, \kappa_z)$ (m^3)	spatial spectrum of the refractive-index fluctuations;
$\Psi_{D,S,T}(\mathbf{x}, z, t)$ [(W m^{-2})$^{1/2}$	total detector field, backscattered field, and transmitted field;
Ω (sr)	solid angle of the effective receiver aperture viewed from the target.

We acknowledge many helpful discussions with R. M. Hardesty, S. W. Henderson, M. J. Post, B. J. Rye, J. H. Shapiro, and R. Targ. This work was partially supported by the National Science Foundation under grant ECS-8819375 and by NASA Marshall Space Flight Center under contract NAS8-37580 (W. D. Jones, technical monitor).

References

1. R. T. H. Collis and P. B. Russell, "Lidar measurements of particles and gases by elastic backscattering and differential absorption," in *Laser Monitoring of the Atmosphere*, E. D. Hinkley, ed. (Springer-Verlag, Berlin, 1976), Chap. 4.
2. R. M. Measures, *Laser Remote Sensing. Fundamentals and Applications* (Interscience, New York, 1984).
3. W. B. Grant, "Laser Remote Sensing Techniques," in *Laser Spectroscopy and Its Applications*, L. J. Radziemski, R. W. Solarz, and J. A. Paisner, eds. (Dekker, New York, 1987), Chap. 8.
4. R. M. Measures, "Fundamentals of Laser Remote Sensing," in *Laser Remote Chemical Analysis*, R. M. Measures, ed. (Wiley, New York, 1988), Chap. 1.
5. R. Targ, M. J. Kavaya, R. M. Huffaker, and R. L. Bowles, "Coherent lidar airborne windshear sensor: performance evaluation," Appl. Opt. **30,** 2013–2026 (1991).
6. R. M. Huffaker, T. R. Lawrence, M. J. Post, J. T. Priestley, F. F. Hall, Jr., R. A. Richter, and R. J. Keeler, "Feasibility studies for a global wind measuring satellite system (Windsat): analysis of simulated performance," Appl. Opt. **23,** 2523–2536 (1984).
7. R. G. Beranek, J. W. Bilbro, D. E. Fitzjarrald, W. D. Jones, V. W. Keller, and B. S. Perrine, "Laser atmospheric wind sounder (LAWS)," in *Laser Applications in Meteorology and Earth and Atmospheric Remote Sensing*, M. M. Sokoloski, ed., Proc. Soc. Photo-Opt. Instrum. Eng. **1062,** 234–248 (1989).
8. R. T. Menzies., "Laser heterodyne detection techniques," Chap. 7 in Ref. 1.
9. J. W. Goodman, "Some effects of target-induced scintillation on optical radar performance," Proc. IEEE **53,** 1688–1700 (1965)
10. A. E. Siegman, "The antenna properties of optical heterodyne receivers," Proc. IEEE **51,** 1350–1358 (1966).
11. D. L. Fried, "Optical heterodyne detection of an atmospherically distorted signal wave front," Proc. IEEE **55,** 57–66 (1967).
12. C. M. Sonnenschein, and F. A. Horrigan, "Signal-to-noise relationships for coaxial systems that heterodyne backscatter from the atmosphere," Appl. Opt. **10,** 1600–1604 (1971). A list of unpublished errata for this paper can be obtained from the present authors.
13. T. R. Lawrence, D. J. Wilson, C. E. Craven, I. P. Jones, R. M. Huffaker, and J. A. L. Thomson, "A laser velocimeter for remote wind sensing," Rev. Sci. Instrum. **43,** 512–518 (1972).

14. H. T. Yura, "Optical heterodyne signal power obtained from finite sized sources of radiation," Appl. Opt. **13,** 150–157 (1974).
15. H. T. Yura, "Signal-to-noise ratio of heterodyne lidar systems in the presence of atmospheric turbulence," Opt. Acta **26,** 627–644 (1979).
16. B. J. Rye, "Antenna parameters for incoherent backscatter heterodyne lidar," Appl. Opt. **18,** 1390–1398 (1979).
17. R. L. Schwiesow, and R. F. Calfee, "Atmospheric refractive effects on coherent lidar performance at 10.6 μm," Appl. Opt. **18,** 3911–3917 (1979).
18. B. J. Rye, "Refractive-turbulence contribution to incoherent backscatter heterodyne lidar returns," J. Opt. Soc. Am. **71,** 687–691 (1981).
19. J. H. Shapiro, B. A. Capron, and R. C. Harney, "Imaging and target detection with a heterodyne-reception optical radar," Appl. Opt. **20,** 3292–3313 (1981).
20. S. F. Clifford and S. Wandzura, "Monostatic heterodyne lidar performance: the effect of the turbulent atmosphere," Appl. Opt. **20,** 514–516 (1981); Appl. Opt. **20,** 1502(E) (1981).
21. R. M. Hardesty, R. J. Keeler, M. J. Post, and R. A. Richter, "Characteristics of coherent lidar returns from calibration targets and aerosols," Appl. Opt. **20,** 3763–3769 (1981).
22. J. Y. Wang, "Heterodyne laser radar SNR from a diffuse target containing multiple glints," Appl. Opt. **21,** 464–475 (1982).
23. B. J. Rye, "Primary aberration contribution to incoherent backscatter heterodyne lidar returns," Appl. Opt. **21,** 839–844 (1982).
24. J. Salzman and A. Katzir, "Signal-to-noise ratio of heterodyne detection: matrix formalism," Appl. Opt. **22,** 888–890 (1983).
25. J. Salzman and A. Katzir, "Heterodyne detection SNR: calculations with matrix formalism," Appl. Opt. **23,** 1066–1074 (1984).
26. L. Lading, S. Hanson, and A. S. Jensen, "Diffraction-limited lidars: the impact of refractive turbulence," Appl. Opt. **23,** 2492–2497 (1984).
27. R. Murty, "Refractive turbulence effects on truncated Gaussian beam heterodyne lidar," Appl Opt. **23,** 2498–2502 (1984).
28. R. M. Hardesty, "Coherent DIAL measurement of range-resolved water vapor concentration," Appl. Opt. **23,** 2545–2553 (1984).
29. J. Y. Wang, "Detection efficiency of coherent optical radar," Appl. Opt. **23,** 3421–3427 (1984).
30. J. Y. Wang, "Lidar signal fluctuations caused by beam translation and scan," Appl. Opt. **25,** 2878–2885 (1986).
31. C. J. Leader, "Speckle effects on coherent laser radar detection efficiency," Opt. Eng. **25,** 644–649 (1986).
32. J. Y. Wang, "Optimum truncation of a lidar transmitted beam," Appl. Opt. **27,** 4470–4474 (1988).
33. Y. Zhao, M. J. Post, and R. M. Hardesty, "Receiving efficiency of pulsed coherent lidars. 1: Theory," Appl. Opt. **29,** 4111–4119 (1990).
34. Y. Zhao, M. J. Post, and R. M. Hardesty, "Receiving efficiency of pulsed coherent lidars. 2: Applications," Appl. Opt. **29,** 4120–4132 (1990).
35. C. A. DiMarzio and C. S. Lins, "Heterodyne SNR computations using orthogonal functions," in *Fifth Conference on Coherent Laser Radar: Technology and Applications,* J. W. Bilbro and C. Werner, eds., Proc. Soc. Photo-Opt. Instrum. Eng. **1181,** 176–185 (1989).
36. J. A. Thomson and F. P. Boynton, "Development of design procedures for coherent lidar measurements of atmospheric winds," Final Rep., contract NOAA-03-7-022-35106, Rep. PD-B-77-137 (Physical Dynamics, Berkeley, Calif., June 1977, revised Sept. 1977, Nov. 1977, and Jan. 1978).
37. R. M. Huffaker, Coherent Technologies, Coherent Technologies, Inc., 3300 Mitchell Lane, Boulder, Colo. 80301 personal communication (1989).
38. M. J. Kavaya, S. W. Henderson, J. R. Magee, C. P. Hale, and R. M. Huffaker, "Remote wind profiling with a solid-state Nd:YAG coherent lidar system," Opt. Lett. **14,** 776–778 (1989).
39. M. Ross, *Laser Receivers. Devices, Techniques, Systems* (Wiley, New York, 1966).
40. M. Ross, ed., Laser Applications (Academic, New York, 1971, 1974), Vols. 1 and 2.
41. B. M. Watrasiewicz and M. J. Rudd, *Laser Doppler Measurements* (Butterworth, London, 1976).
42. C. G. Bachman, *Laser Radar Systems and Techniques* (Artech House, Dedham, Mass., 1979).
43. L. E. Drain, *The Laser Doppler Technique* (Wiley-Interscience, Chichester, England, 1980).
44. D. K. Killinger and A. Mooradian, eds., *Optical and Laser Remote Sensing* (Springer-Verlag, Berlin, 1983).
45. V. E. Zuev and I. E. Naats, *Inverse Problems of Lidar Sensing of the Atmosphere* (Springer-Verlag, Berlin, 1983).
46. T. Kobayashi, "Techniques for laser remote sensing of the environment," Remote Sensing Rev. **3,** 1–56 (1987).
47. D. K. Killinger and N. Menyuk, "Laser remote sensing of the atmosphere," Science **235,** 37–45 (1987).
48. V. A. Banakh and V. L. Mironov, *Lidar in a Turbulent Atmosphere* (Artech House, Dedham, Mass., 1987).
49. R. L. Schwiesow and R. E. Cupp, "Calibration of a cw infrared Doppler lidar," Appl. Opt. **19,** 3168–3172 (1980).
50. R. Foord, R. Jones, J. M. Vaughan, and D. V. Willetts, "Precise comparison of experimental and theoretical SNRs in CO_2 laser heterodyne systems," Appl. Opt. **22,** 3787–3795 (1983).
51. J. H. Shapiro, "Precise comparison of experimental and theoretical SNRs in CO_2 laser heterodyne systems: comments," Appl. Opt. **24,** 1245–1247 (1985).
52. J. L. Meyzonnette, B. Remy, and G. Saccomani, "Imaging CO_2 laser radar with chirp pulse compression," in *Laser Radar II,* R. J. Becherer and R. C. Harney, eds., Proc. Soc. Photo-Opt. Instrum. Eng. **783,** 169–179 (1987).
53. C. W. Helstrom, "Detectability of coherent optical signals in a heterodyne receiver," J. Opt. Soc. Am. **57,** 353–361 (1967).
54. L. Mandel and E. Wolf, "Optimum conditions for heterodyne detection of light," J. Opt. Soc. Am. **65,** 413–420 (1975).
55. J. J. Degnan and B. J. Klein, "Optical antenna gain 2: Receiving antennas," Appl. Opt. **13,** 2397–2401 (1974).
56. D. Fink, "Coherent detection signal-to-noise," Appl. Opt. **14,** 689–690 (1975).
57. S. C. Cohen, "Heterodyne detection: phase front alignment, beam spot size, and detector uniformity," Appl. Opt. **14,** 1953–1959 (1975).
58. D. Fink and S. N. Vodopia, "Coherent detection SNR of an array of detectors" Appl. Opt. **15,** 453–454 (1976).
59. T. Takenaka, K. Tanaka, and O. Fukumitsu, "Signal-to-noise ratio in optical heterodyne detection for Gaussian fields," Appl. Opt. **17,** 3466–3471 (1978).
60. N. Saga, K. Tanaka, and O. Fukumitsu, "Diffraction of a Gaussian beam through a finite aperture lens and the resulting heterodyne efficiency," Appl. Opt. **20,** 2827–2831 (1981).
61. K. Tanaka and N. Saga, "Maximum heterodyne efficiency of optical heterodyne detection in the presence of background radiation," Appl. Opt. **23,** 3901–3904 (1984).
62. K. Tanaka and N. Ohta, "Effects of tilt and offset of signal field on heterodyne efficiency," Appl. Opt. **26,** 627–632 (1987).
63. V. U. Zavorotnyi, V. I. Klyatskin, and V. I. Tatarskii, "Strong fluctuations of the intensity of electromagnetic waves in randomly inhomogeneous media," Zh. Eksp. Teor. Fiz. **73,** 481–497 (1977) [Sov. Phys. JETP **46,** 252–260 (1977)].

64. R. Dashen, "Path integrals for waves in random media," J. Math. Phys. **20,** 894–920 (1979).
65. V. I. Tatarskii and V. U. Zavorotnyi, "Strong fluctuations in light propagation in a randomly inhomogeneous medium," in *Progress in Optics,* E. Wolf, ed. (North-Holland, Amsterdam, 1980), Vol. 28.
66. S. M. Flatté, "Wave propagation through random media: contributions from ocean acoustics," Proc. IEEE **71,** 1267–1294 (1983).
67. J. L. Codona, D. B. Creamer, S. M. Flatté, R. G. Frehlich, and F. S. Henyey, "Moment-equations and path-integral techniques for wave propagation in random media," J. Math. Phys. **27,** 171–177 (1986).
68. J. L. Codona, D. B. Creamer, S. M. Flatté, R. G. Frehlich, and F. S. Henyey, "Solution for the fourth moment of waves propagating in random media," Radio Sci. **21,** 929–948 (1986).
69. J. L. Codona and R. G. Frehlich, "Scintillation from extended incoherent sources," Radio Sci. **22,** 469–480 (1987).
70. R. G. Frehlich, "Space-time fourth moment of waves propagating in random media," Radio Sci. **22,** 481–490 (1987).
71. G. M. Ancellet and R. T. Menzies, "Atmospheric correlation-time measurements and effects on coherent Doppler lidar," J. Opt. Soc. Am. A **4,** 367–373 (1987).
72. K. M. van Vliet, "Noise limitations in solid state detectors," Appl. Opt. **6,** 1145–1169 (1967).
73. J. M. Hunt, J. F. Holmes, and F. Amzajerdian, "Optimum local oscillator levels for coherent detection using photoconductors," Appl. Opt. **27,** 3135–3141 (1988).
74. J. H. Shapiro, "Reciprocity of the turbulent atmosphere," J. Opt. Soc. Am. **61,** 492–495 (1971).
75. M. J. Kavaya, R. T. Menzies, D. A. Haner, U. P. Oppenheim, and P. H. Flamant, "Target reflectance measurements for calibration of lidar atmospheric backscatter data," Appl. Opt. **22,** 2619–2628 (1983).
76. M. J. Kavaya and R. T. Menzies, "Lidar aerosol backscatter measurements: systematic, modeling, and calibration error considerations," Appl. Opt. **24,** 3444–3453 (1985).
77. M. J. Kavaya, "Polarization effects on hard target calibration of lidar systems," Appl. Opt. **26,** 796–804 (1987).
78. R. L. Fante, "Wave propagation in random media: A systems approach," in *Progress in Optics,* E. Wolf, ed. (North-Holland, Amsterdam, 1985), Vol. 22, pp. 341–398.
79. V. A. Banakh and V. L. Mironov, "Phase approximation of the Huygens–Kirchhoff method in problems of laser-beam propagation in the turbulent atmosphere," Opt. Lett. **1,** 172–174 (1977).
80. S. M. Wandzura, "Meaning of quadratic structure functions," J. Opt. Soc. Am. **70,** 745–747 (1980).
81. V. I. Tatarskii, *The Effects of the Turbulent Atmosphere on Wave Propagation* (Keter, Jerusalem, 1971).
82. V. U. Zavorotnyi, "Strong fluctuations of electromagnetic waves in a random medium with finite longitudinal correlation of the inhomogeneities," Zh. Eksp. Teor. Fiz. **75,** 56–65 (1978) [Sov. Phys. JETP **48,** 27–31 (1978)].
83. W. A. Coles and R. G. Frehlich, "Simultaneous measurements of angular scattering and intensity scintillations in the atmosphere," J. Opt. Soc. Am. **72,** 1041–1048 (1982).
84. J. H. Churnside and S. F. Clifford, "Log-normal Rician probability density function of optical scintillations in the turbulent atmosphere," J. Opt. Soc. Am. A **4,** 1923–1930 (1987).
85. R. G. Frehlich, "Intensity covariance of a point source in a random medium with a Kolmogorov spectrum and an inner scale of turbulence," J. Opt. Soc. Am. A **4,** 360–366 (1987).
86. R. L. Fante, "Inner-scale size effect on the scintillations of light in the turbulent atmosphere," J. Opt. Soc. Am. **73,** 277–281 (1983).
87. L. D. Dickson, "Characteristics of a propagating Gaussian beam," Appl. Opt. **9,** 1854–1861 (1970).
88. M. Born and E. Wolf, *Principles of Optics* (Pergamon, London, 1980).
89. D. U. Fluckiger, R. J. Keyes, and J. H. Shapiro, "Optical autodyne detection: theory and experiment," Appl. Opt. **26,** 318–325 (1987).
90. R. G. Frehlich, "Conditions for optimal performance of monostatic coherent laser radar," Opt. Lett. **15,** 643–645 (1990).
91. T. J. Kane, B. Zhou, and R. L. Byer, "Potential for coherent Doppler wind velocity lidar using neodymium lasers," Appl. Opt. **23,** 2477–2481 (1984).